https://dx.doi.org/10.1016/j.aei.2021.101403

Post disaster adaptation management in airport: a coordination of runway and hangar resources for relief cargo transports

Yichen QIN[a], Kam K.H. NG[b,*], Hongtao HU[c,**],Felix T.S. CHAN[d], Shichang XIAO[c]

[a] *School of Economics and Management, Shanghai Maritime University, Shanghai, China, 201306*

[b] *Department of Aeronautical and Aviation Engineering, The Hong Kong Polytechnic University, Hung Hom, Hong Kong SAR, China*

[c] *Logistics Engineering College, Shanghai Maritime University, Shanghai, China, 201306*

[d] *Department of Industrial and Systems Engineering, The Hong Kong Polytechnic University, Hung Hom, Hong Kong SAR, China*

*Corresponding author: kam.kh.ng@polyu.edu.hk (Kam K.H. NG),
** Corresponding author: hthu@shmtu.edu.cn (Hongtao HU)
Yichen QIN: ycqin@shmtu.edu.cn
Felix T.S. CHAN: f.chan@polyu.edu.hk
Shichang XIAO: scxiao@shmtu.edu.cn

Acknowledgement

The research is supported by the School of Economics and Management, Shanghai Maritime University; and the Department of Aeronautical and Aviation Engineering, The Hong Kong Polytechnic University. Our gratitude is also extended to The Natural Science Foundation of China (Grant No. 71971143 and 71771143); and the Research Committee and the Department of Aeronautical and Aviation Engineering, The Hong Kong Polytechnic University for support of the project (UALL, BE3V); and the Soft Science Key Project of Shanghai Science and Technology Innovation Action Plan (Grant No. 20692193300).

Post disaster adaptation management in airport: a coordination of runway and hangar resources for relief cargo transports

Abstract

Air traffic congestions for processing relief cargos under post-disaster relief scenarios are common, due to high transport demands within a short time. To enhance the resilience of relief operations at airport, an optimization problem of relief air cargo transportations involving aircraft sequencing and loading/unloading within a designated hangar is studied in this paper. The objective is minimizing the tardiness in fulfilling inbound and outbound relief cargos. A mixed-integer linear programming model is formulated, which incorporates aircraft sequencing and hangar parking planning. To resolve the practical problem efficiently, we propose a two-stage optimization approach, which reduces complexity in solving the original model by coordinating the decisions of aircraft landing and take-off schedule and cargo hangar parking arrangement through iterations. The efficiency of the proposed method is examined through the computational results. High-quality solutions can be obtained by the two-stage optimization method within a reasonable time for practical implementation, which enhances the responsiveness and resource utilization of airport operations management under disaster relief situations.

Keywords: Post-disaster relief, Aircraft sequencing and scheduling problem, Hangar parking arrangement, Adaptive decision-making, Airport management

1. Introduction

Relief cargo transportation is one of the most significant components in disaster recovery and emergency response, and the timeliness of delivery is primal goal in any kind of disaster/post-disaster restorations [1]. Recently, disaster relief logistics planning and optimization problems under different context and scenarios have been investigated, including road restoration [2], logistics service network design for humanitarian response [3], location-transportation with vehicle routing [4, 5] and engineering rescue tasks scheduling [6, 7]. Given its speediness and flexibility, intercity and international air transport becomes indispensable ways of urgent supply within a short time. In this regard, air traffic congestion on runway and ground operations is common due to concentrated demands within a short time [8, 9]. The implementation of efficient and responsive traffic and cargo turnover strategy is prerequisite in mitigating the negative impacts of loss and damage.

The emerging optimization methods for the adaptive decision-making by coordinating the airside and landside operations can provide a holistic view of relief cargo transportation and adapt to the environmental changes [10, 11]. From the perspective of airside and landside operations at an airport, arranging the relief cargo transportation for mission aircraft includes runway scheduling and aircraft parking stand planning for each arrival and departure along the planning period [12]. Airport runway scheduling (also known as aircraft sequencing problem) determines a series of aircraft's landing and departure sequence in order to better utilize the limited runway resource, with consideration of safety separation between two aircraft on the runway. An aircraft parking stand assignment problem concerns a group of arriving aircraft's parking arrangements to maximize use of the limited space within the designated area. The parking stand in an airport includes the gate connecting to the terminal building, aprons near the terminal building, as well as aircraft hangar with cover. For the mission aircraft in post-disaster relief, their parking positions are usually assigned to hangar for cargo loading and unloading.

Given the concentrated demands for disaster relief transportations, congestion of aircraft pending for arrival and departure occurs within a short time. In this connection, runway and cargo hangar are highly utilized, and the airport is not necessarily able to process all inbound and outbound relief mission flight demands. Some flights are forced to cancel or delay their missions due to the unavailability of runway and hangar resources, which can be commonly witnessed under different post-disaster relief scenarios in different places over the world. Seeing the incoordination-caused bottlenecks in airport resources distribution under crisis relief situations, this paper focuses on enhancing the efficiency of mission flights operations associated with an airport in order to enhance its capacity. Therefore, the aircraft sequencing and hangar parking stand arrangements are considered simultaneously under disaster-relief scenarios.

According to heterogeneous mission flight plans, the coordination of runway and hangar operations facilitates the loading and unloading tasks for mission aircraft, so as to enhance the turnover rate for limited mission fleet and avoid unnecessary congestions and blockage on air traffic and hangar operations. Therefore, aircraft sequencing problem and hangar parking planning with heterogeneous specifications and missions are studied in the model. One of the major tasks under disaster relief scenarios is to develop a systematic schedule involving air and ground operations, including the landing and departure schedule, in addition to hangar parking plans for relevant cargo processing of all mission flights. Along the planning horizon, the landing time, hangar moving in/out time, and the departure time for each mission aircraft is determined and optimized in the integrated model. Optimizing mission aircraft's air and ground operations is challenging because: (1) runway separation arrangement is required between two consecutive flights, and is subjected to changes according to various aircraft specification; (2) flexible hangar parking stand arrangement is needed to maximize the utilization of limited space given the differences in physical size and dimensions of mission aircraft moving into the hangar for cargo processing; (3) aircraft movements in cargo-processing hangar need to be carefully modelled and considered, as the mission time window varies among mission flights and blockages on movements should be minimized. The main contributions of this paper include: (1) Development of a systematic Mixed-Integer Linear Programming (MILP) model that integrates the abovementioned critical factors in mission flight arrangement; (2) Flexible hangar space arrangement practice that is adopted to enhance the utilization of limited space; (3) An enhanced discrete-time mathematical model that reduces the complexity of the discrete-time based MILP model ; and (4) A high-quality near-optimal solution to the proposed problem within a reasonable time.

We organize the remainder of this paper as follows: a comprehensive literature review covering the research background, problem nature and research gap is provided in Section 2. The problem description and mathematical model formulation are presented in Section 3. Afterward, the procedures of the proposed two-stage optimization approach are discussed in Section 4. Computational experiment and results are presented and discussed in Section 5, followed by the conclusions in Section 6.

2. Literature review

In order to highlight the difference between the current study and other relevant research works, the literature review is presented in regard to two major considerations in mission flight planning framework at airport under disaster relief scenarios: aircraft sequencing and parking planning.

2.1 Aircraft sequencing and scheduling problem (ASSP)

Runway capacity has been a major bottleneck in air traffic control, and its enhancement has attracted the attention of relevant fields recently in order to maintain efficient operations at airports. Planning of aircraft landing and departure procedures is the core component in runway operations. ASSP is modelled from a microscopic view of the overall air traffic flow structure, which is constrained by the runway resource, safety consideration and the utilization of runway system [13-16]. In literature, runway operations planning is classified into aircraft landing planning, departure planning and mixed operating mode planning problems. Mixed-mode operations is a generalized version of runway operations, which allows landing/departure for a pair of consecutive flights using the same runway [17]. The objective function in ASSP formulation varies, including makespan minimization [14], overall tardiness minimization [18], as well as average delay minimization. Many variations of First-Come-First-Serve (FCFS) heuristic emerge for adoption of different objective function settings so as to enhance solution quality. In addition, heuristic and meta-heuristic algorithms are proposed, considering the NP-hardness of the problem[13]. Salehipour, Modarres and Naeni [19] developed a hybrid meta-heuristic algorithm by adopting the simulated annealing framework, which is able to obtain optimal solutions for problem instances with more than one hundred aircraft and a high-quality solution for instances with more than 500 aircraft. Academics are now pursuing robust and adaptive decision making (DM) in real-life engineering applications [20, 21]. Ng, Lee, Chan and Qin [22] modified an artificial bee colony algorithm to solve a robust aircraft sequencing and scheduling problem considering deviation of scheduled time, and the proposed method obtained close-to-optimal results with alleviated computational burden in solving one-hour traffic planning scenarios. Salehipour [23] decomposed the original single- and multi-runway aircraft landing problem into a series of solvable subproblems with heuristic, considering the continuous changes in the number of arriving aircraft and the determination of landing schedule within a short window. Sabar and Kendall [24] developed an iterated local search algorithm for the aircraft landing problem, which incorporates a perturbation operator to modify the incumbent solution and escape from local optima. Ng, Lee, Chan, Chen and Qin [25] proposed a two-stage optimization framework to resolve the terminal traffic flow problem in hedging arrival waypoints uncertainty. The integrated traffic flow network and ASSP can also cooperate with the terminal airspace congestion offloading management methods, including aeronautical holding decision [26, 27] and runway configuration planning [28].

2.2 Hangar parking planning

Aircraft parking planning problem is considered with the other decision-makings under different situations and operators in aviation industry [29, 30]. For example, Chen, He, Leung, Lan and Han [31] studied an aircraft maintenance engineering technician's assignment problem with aircraft parking planning for maintenance tasks, assuming that the types of aircraft to be serviced are limited and that hangar parking capacity is constant. Afterwards, Qin, Chan, Chung, Qu and Niu [32] proposed an aircraft parking stand arrangement problem in the context of independent aircraft engineering company providing maintenance checks to aircraft with different physical specifications. Zheng, Yang, He, Wang, Chu and Yu [33] studied an integrated aircraft scheduling/sequencing problem and parking planning under disaster relief scenarios, considering an unfixed-stand parking strategy. A hybrid simulated annealing and reduced variables neighborhood search algorithm was proposed to obtain high quality solutions for large scale problem instances. The aircraft parking planning problem addressed in this paper under disaster relief context is similar to dynamic layout planning problems covering multiple period, since space for placing facilities is temporarily occupied by different objects according to their respective time windows. For example, integration of two-dimension cargo pick-up and deliver constraints into the vehicle routing problem is a typical routing-packing problem [34]. In such a problem, the decision-makings involve vehicle routing and placing goods in the respective vehicle under two-dimensional environment to satisfy customer scattered at different delivery/pick-up points [35, 36]. Considering the Last-In-First-Out discipline adopted in practice, the common objective of the problem includes minimizing position rearrangements of goods through the entire route, which avoids unnecessary tardiness in fulfilling the demands associated with their time windows [34, 35, 37-39]. Such extension of VRP is similar to the aircraft parking layout planning problem in hangar. Though extensive research works covering different industrial/academic fields exist [40-45], most of the correlated dynamic layout planning approaches are not compatible to resolve the aircraft parking planning problem addressed in this paper. The specific considerations of aircraft parking planning include: (a) irregular physical shapes of aircraft and their modelling in a mathematical model; (b) flexible Last-In-First-Out strategy with the tolerance of tardiness while fulfilling the loading/unloading cargo tasks; (c) aircraft movement path blocking and its impact on timeliness in completing cargo processing tasks.

When modelling aircraft as irregular polygons in two-dimensional space, No-Fit Polygon (NFP) is a widely adopted tool in preventing irregular polygons from overlapping in a geometrical space. Regarding the generation of No-Fit Polygons, detailed instructions were provided by Bennell and Oliveira [46] and Bennell and Oliveira [47]. To incorporate NFP into the mathematical model, a horizontal slices formulation approach was formulated by Alvarez-Valdes, Martinez and Tamarit [48], which was enhanced based on the foundation provided by Fischetti and Luzzi [49]. Moreover, guillotine cuts were considered by Martinez-Sykora, Alvarez-Valdes, Bennell and Tamarit [50] in their MIP model with horizontal slicing approach. To enhance the robustness of the mathematical model in processing irregular non-convex polygons, two robust mixed-integer formulations were developed by Cherri, Mundim, Andretta, Toledo, Oliveira and Carravilla [51], which incorporate decomposition of the original complex polygon into several simple (convex) polygons to generate NFP.

3. Problem description and mathematical model formulations

3.1 Problem description

In this problem, we aim to accommodate relief cargo flights in an airport by allocating the runway and cargo hangar resources in an integrated manner at the strategic decision level (several days in advance) based on their importance and urgency. The cargo flights take priority over the other ordinary passenger flights in runway scheduling, though the ordinary passenger flights take a large portion of the entire operational volume. Regarding the practices of cargo flight accommodation, the congestions of cargo flights arrival are mainly reflected on hangar operations. Different from the congestions on a runway, cargo hangar congestion can last for a relatively longer period of time, determined by the length of cargo processing time (also cargo parking space occupation time). As the cargo processing time of each cargo flight can last from a dozen to hundreds of hours, the planning horizon of each problem instances is mainly subjected to the estimated time of arrival and the cargo processing time. In this regard, the planning horizon (time frame) ranges from days to weeks, according to the mission specifications of cargo flights.

One of the main purposes of integration at strategic level is to avoid creating bottlenecks in runway scheduling, ensuring that the necessary resources are allocated to these flights in a timely manner. For cargo flights, hangar resource is the most critical one in post disaster relief planning. Integration coordinates the runway scheduling with hangar planning, thus avoiding wastage of hangar resource, in addition to hangar operation delays caused by the incoordination between runway scheduling and hangar planning. It is possible to make runway scheduling decisions at the tactical level. Nevertheless, the deviation of runway assignments, landing and take-off time schedule for cargo flights may delay the operations in cargo hangar. In this regard, the integration assures that the runway resource is allocated to the cargo flight at a higher priority over the other normal flights.

The runway scheduling and relief aircraft parking problem studies the process of aircraft sequencing and landing schedule on the runway, and the parking arrangement for relief cargo loading and unloading at the hangar, which is shown in Figure 1. Specifically, each mission aircraft has its cargo delivery or shipment mission at the airport, associated with an estimated time of arrival and the cargo loading/unloading processing time. The relief cargo process hangar is a covered facility with fixed dimensions (length and width). The overall objective of the problem is to minimize the turnaround time and tardiness for all mission flights by optimizing runway and hangar resource utilizations, which facilitates the implementation of relief cargo processing.

The airport operations under post-disaster relief scenarios involves runway and hangar operations for incoming mission flights, which is shown in Figure 2. The landing time, take-off time associated with operating runways and parking position are coordinated and arranged for each incoming mission flight. Regarding the operations in the cargo hangar, the transitions of cargo hangar layout for mission aircraft parking specify the position occupied by different mission flights along the entire planning period. Due to the heterogenous physical configurations of incoming mission aircraft, the parking stand positions in the cargo hangar are not prefixed and standardized, which enhances the flexibility of hangar space utilization. The upward and downward arrows denote the moving operations of mission aircraft in the cargo hangar.

The contributions of the problem include: 1) adoption of flexible aircraft parking stand strategy in the cargo hangar, which is modelled in a two-dimensional space; 2) integration of the airport runway sequencing/scheduling problem and the cargo hangar parking stand arrangement problem, which aims to better utilize the limited airport resources under the post-disaster relief scenario; 3) formulation of a Mixed-Integer Linear Programming model with two-dimensional constraints for cargo hangar arrangement and 4) a two-stage optimization method designed to enhance the airside and ground side resource utilization and operation, which facilitates to obtain high quality solutions within a reasonable time for practical use.

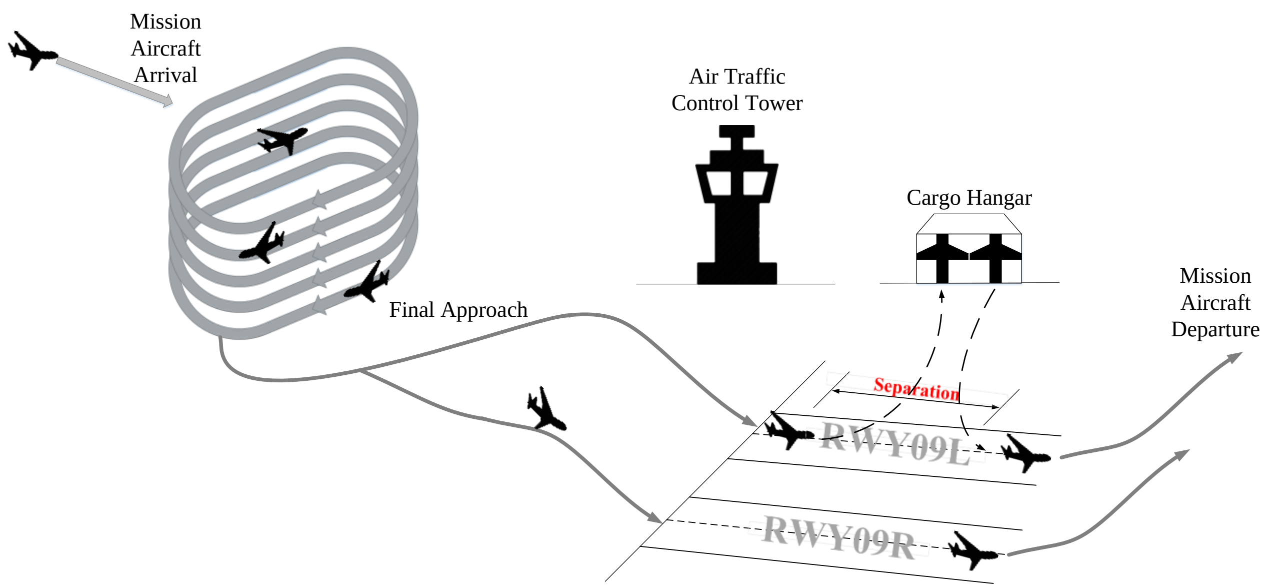

Figure 1 Airport operations under post disaster scenarios for relief cargo transports

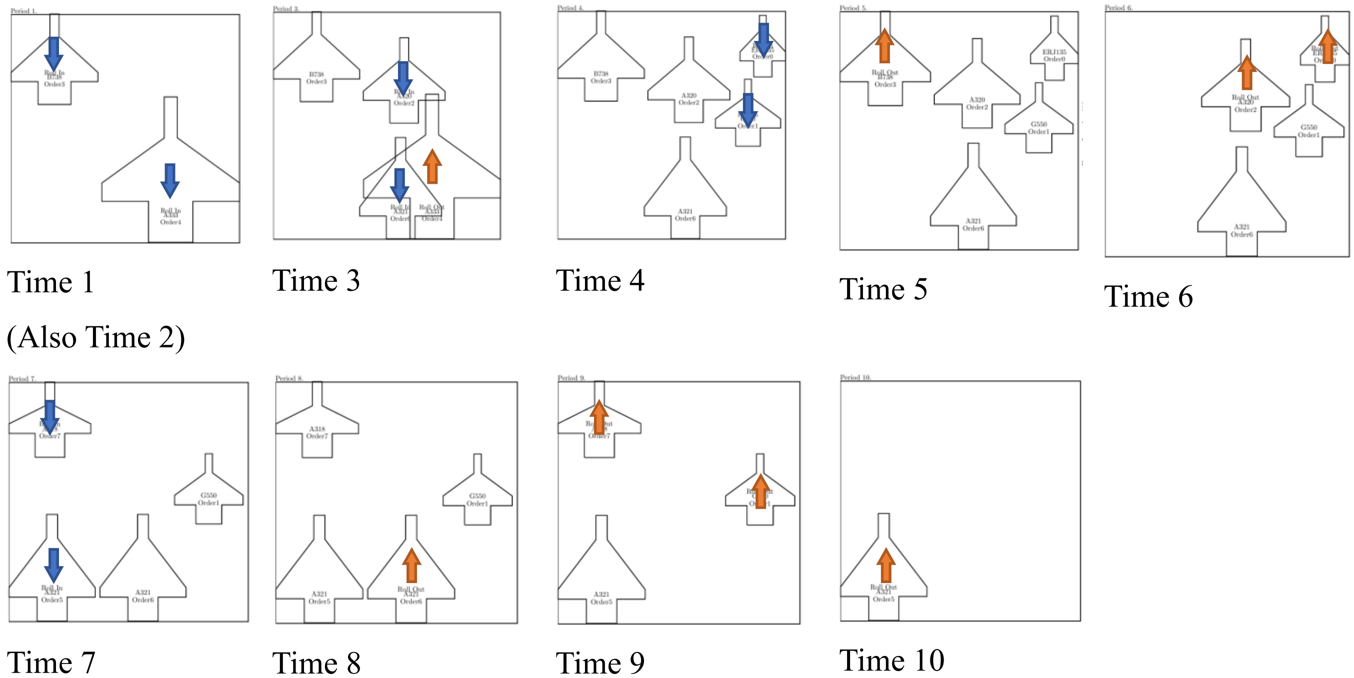

Figure 2 The mission aircraft runway scheduling and cargo hangar arrangement problem

3.2 The development of non-overlapping constraints for cargo hangar parking

We considered modelling aircraft according to their actual physical shapes in the mathematical model, which aims to make the best the utilization of limited hangar space under the relief scenario. The space wastage of modelling aircraft as rectangle in two-dimensional space is shown in Figure 3. To enhance the utilization of limited hangar space, modelling aircraft as non-convex polygon is an attractive option. In this regard, the method of preventing the modelled aircraft, i.e., non-convex polygons, from overlapping in two-dimensional space becomes one of the significant elements in mathematical modelling. The conventional linear constraint is not able to describe the complex geometrical relations between a pair of non-convex polygons. To overcome this limitation, we adopt No-Fit Polygon between a pair of polygons, a widely adopted approach in the nesting problem in literature, in the development of mathematical model to generate non-overlapping constraints. As shown in Figure 3, let the middle point at the rear end of the aircraft be a reference point denoting its coordinates (x_i, y_i) in two-dimensional space. The No-Fit Polygon (NFP_{ij}) between a pair of aircraft p_i and p_j prescribes the restricted region that aircraft p_j 's coordinate cannot be placed in to avoid overlapping between two aircraft, under the condition that aircraft p_i is the stationary one while aircraft p_j is the moving one. The feasible region for placing relative movable aircraft p_j is the region outside NFP_{ij}. We use two simple polygons to illustrate the idea of obtaining *NPF*. As shown in Figure 4, the *NFP* between polygons P_1 and P_2 is generated by tracing the path of the reference point on P_2. By keeping P_2 sliding around the boundary of P_1, two polygons always touch with each other but never overlap. The same logic applies to the generation of *NFP* between two aircraft (Figure 5 (a)). Detailed tutorials for generating No-Fit Polygon between a pair of polygons are provided in Bennell and Oliveira [46] and Bennell and Oliveira [47].

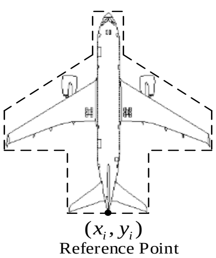

Figure 3 Geometric representation and reference point of aircraft

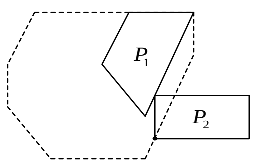

Figure 4 No-Fit Polygon generation for two simple polygons

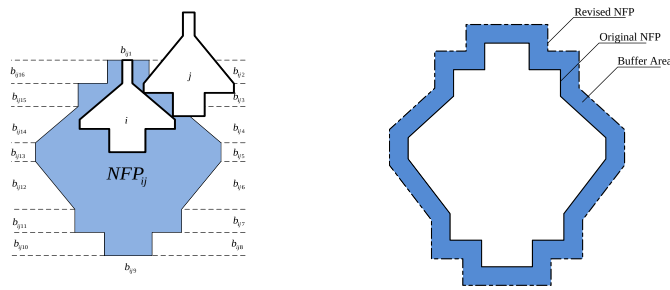

(a) (b)

Figure 5 Horizontal slices outside *NFP* of a pair of aircraft

To transform the geometrical information of *NFP* into a linear programming model, Alvarez-Valdes, Martinez and Tamarit [48] proposed a horizontal slicing Mixed-Integer Linear Programming (MILP) model, which divides the region outside *NFP* into multiple horizontal slices. Specifically, a horizontal slice is created by drawing horizontal lines from vertex of *NFP*, as shown in Figure 5 (a). The geometrical information of one slice is provided by the segment of *NFP* and the horizontal slices. Afterwards, a binary variable b_{ijk} is assigned to denote the reference point's position of the relative movable aircraft. If the relative movable aircraft p_j's coordinates are assigned to be within the area of horizontal slice k, then the value of binary variable will be $b_{ijk} = 1$. A general form of the linear constraint preventing overlapping can be expressed as :

$\alpha_{ij}^{kf}(x_j - x_i) + \beta_{ij}^{kf}(y_j - y_i) \le q_{ijk} + M \cdot (1 - b_{ijk}),\ \forall i, j \in P, i \ne j, k = 1, 2, ..., m_{ij}$. The linear equation

$\alpha_{ij}^{kf}(x_j - x_i) + \beta_{ij}^{kf}(y_j - y_i) = q_{ijk}$ denotes the geometrical information of the f^{th} edge of the k^{th} slice in NFP_{ij}, where m_{ij} is the total number of horizontal slices outside the NFP_{ij}. Specifically, to describe the geometrical information of those horizontal slices in a mathematical model, we need to record the slope and intercept of each edge of slice. After transforming the linear expression to a general form, α, β and q are used to describe the slope and intercept of each edge. M is a sufficiently large number, which is used to control the activation/deactivation of the non-overlapping constraint. Specifically, the coordinates of a relative movable aircraft (in this case, aircraft j) must be put in one of the horizonal slices, so as to prevent overlapping. Furthermore, having two aircraft touch with each other is not allowed in practical situations. Therefore, a buffer area should be imposed as a safety margin between each pair of aircraft. In this regard, we revise the edge of original *NFP* by moving each segment of *NFP* outward to distance n (as shown in Figure 5 (b)), which expands the restricted area of the coordinates of the relative movable aircraft p_j. To further enhance the hangar space utilization, three-dimensional non-overlapping constraints are further incorporated in the mathematical model, which is developed based on the above mentioned No-Fit Polygon method. We refer interested readers to [52], for the detailed explanation of the three-dimensional non-overlapping constraints.

3.3 Mixed-Integer Linear Programming model

3.3.1 Model assumptions

The assumptions of the mathematical model formulation under disaster relief scenarios are as follows.

- The target arrival and departure time of the mission flight are assumed to be deterministic;
- The relief cargo loading and unloading processing time are stable and predetermined;
- Aircraft’s turnaround time is relatively short, which can be combined with the cargo processing time;
- Aircraft’s landing, taxi & roll-in, cargo unloading, loading, roll-out & taxi-out, and departure time are relatively short, which can be absorbed in cargo processing time.
- The parking position of each mission aircraft cannot be adjusted during the cargo processing period;
- The mission aircraft can be released for departure once the cargo processing task has been finished;

- The moving in or moving out operations of an aircraft cannot commence if its movement path is blocked by any existing aircraft in the hangar;
- The movement path of all mission aircraft is a straight line, turning movements are not allowed in the cargo hangar for safety assurance;
- After landing on the runway, the mission aircraft may not necessarily be able to move into the cargo processing hangar if the hangar is operating at its full capacity.

3.3.2 Parameters and decision variables

The parameters involved in the mathematical model include the geometrical and timeliness information:

- The timeliness of each mission flight, which includes the aircraft type, relief cargo unloading/loading processing lead time, estimated time of arrival (ETA) to the airport, and estimated time of departure (ETD);
- The two-dimensional geometrical information of aircraft, which includes the physical specifications and dimensions, as well as the No-Fit Polygon between each pair of aircraft;
- The separation time between two consecutive aircraft on the same runway;
- The dimensions of the cargo processing hangar.

The list of notations for parameters mentioned above are as follows:

Notations

$TGAT_i$	Target arrival time of mission aircraft *i*
$TGDT_i$	Target departure time of mission aircraft *i*
CPT_i	Required cargo processing time (loading/unloading) of mission aircraft *i*
$SepT_{ij}$	The minimum landing/take-off operation separation time on runway between aircraft *i* and *j*
R	Set of runways for landing and departure
a_t	Set of scheduled arrival mission aircraft at time *t*
d_t	Set of schedule departure mission aircraft at time *t*
A_t	Set of cumulative scheduled arrival mission aircraft at the airport from beginning to time *t*. $A_t \in \bigcup_{i=0}^{t} a_t$

D_t	Set of cumulative scheduled departure mission aircraft at the airport from beginning to time *t*. $D_t \in \bigcup_{i=0}^{t} d_t$
A_T	Set of mission aircraft during planning horizon
t	Index of time, where *T* is the length of planning horizon
$TailD_i$	Tail distance of aircraft *i*
$penalty1$	Penalty of rejecting arrival of mission aircraft *i* during planning period
$penalty2$	penalty of late departure of mission aircraft *i* during planning period
$penalty3$	Penalty of failing to dispatch mission flight at the end of planning period
$Weightness_i$	Degree of importance of mission flight *i*
WH	width of hangar
LH	length of hangar
wa_i	width of aircraft *i*
la_i	length of aircraft *i*
NFP_{ij}	*NFP* of aircraft *i* and *j* with minimal safety distance
s_{ij}^{k}	*k*th horizontal slice of the region outside the NFP_{ij}
$\alpha_{ij}^{kf}, \beta_{ij}^{kf}, q_{ij}^{kf}$	parameters used to define the *f*th linear equation of the horizontal slice s_{ij}^{k} outside the NFP_{ij}
m_{ij}	number of slices outside NFP_{ij}
t_{ij}^{k}	number of linear equations used to define the slice s_{ij}^{k}
M	a large number

To determine a mission flight schedule to fulfill the cargo processing and the runway planning during the planning period, we introduce two groups of decision variables, including 1) runway sequencing and scheduling group and 2) aircraft parking arrangement group.

1) Decision variables for flights sequencing and scheduling on runway

RJF_i	1, if mission flight cannot be accommodated within the planning period
MDF_i	1, if mission flight cannot complete cargo handling task within the planning period
$rwyA_{ir}$	1, if aircraft *i* is assigned to runway *r* on arrival; 0, otherwise
$rwyD_{ir}$	1, if aircraft *i* is assigned to runway *r* on departure; 0, otherwise
$sqrAA_{jir}$	1, if aircraft *j* arrives before aircraft *i* arrives on the same runway *r* (not necessary immediately); 0, otherwise

$sqrDD_{jir}$	1, if aircraft *j* departs before aircraft *i* departs on the same runway *r* (not necessary immediately); 0, otherwise
$sqrDA_{jir}$	1, if aircraft *j* departs before aircraft *i* arrives on the same runway *r* (not necessary immediately); 0, otherwise
$sqrAD_{jir}$	1, if aircraft *j* arrives before aircraft *i* departs on the same runway *r* (not necessary immediately); 0, otherwise
$Arrt_{ir}$	The assigned arrival time for aircraft *i* on runway *r*
$Dept_{ir}$	The assigned departure time for aircraft *i* on runway *r*

2) Decision variables for aircraft parking arrangement in cargo hangar

(x_i, y_i)	Coordinates of incoming mission aircraft's position in cargo hangar
$rollout_{it}$	Indicator of the roll out movement operations for mission aircraft *i* at time *t*, and the binary variable takes value 1 if it rolls out at the current time
$rollin_{it}$	Indicator of the roll in movement operations for mission aircraft *i* at time *t*, and the binary variable takes value 1 if it rolls in at the current time
$rollout_{iT^*}$	Indicator of the failure of roll out movement operations for mission aircraft *i*, and the binary variable takes value 1 if the mission aircraft is blocked until the end of planning period
p_{it}	Indicator of parking status of mission aircraft *i*, and the binary variable takes value 1 if the aircraft is in the cargo hangar at time *t*.
h_{ijt}	Indicator of blocking relations between mission aircraft *i* and *j*, and the binary variable takes value 1 if the movement path of aircraft *i* is blocked by aircraft *j* at time *t*
L_{ij}	Indicator of relative position between aircraft *i* and *j*, and the binary variable takes value 1 if aircraft *i* is placed on the left hand side of aircraft *j* without any movement blocking by *j*
R_{ij}	Indicator of relative position between aircraft *i* and *j*, and the binary variable takes value 1 if aircraft *i* is placed on the right hand side of aircraft *j* without any movement blocking by *j*
U_{ij}	Indicator of relative position between aircraft *i* and *j*, and the binary variable takes value 1 if aircraft *i* is placed above aircraft *j* without any movement blocking by *j*
b_{ijkt}	Indicator of relative position between aircraft *i* and *j*, and the binary variable takes value 1 if the coordinates of aircraft *j* is placed in the horizontal slice s_{ij}^k associated with the area outside NFP_{ij} at time *t*, which prevents overlapping between two aircraft

3.3.3 Objective and constraints

$$Minimize \sum_{\forall i \in A_T} Weightness_i \cdot \left[(1 - \sum_{t \geq ETA_i} in_{it}) \cdot penalty1_i + \sum_{t \geq ETD_i} out_{it} \cdot (t - ETD_i) \cdot penalty2_i + out_{iT^*} \cdot penalty3_i \right]$$

To accommodate cargo flights, the goal of this model is to provide a strategic decision (making decision several days in advance before the actual operation) for the runway scheduling and cargo hangar planning problems, considering the duration of cargo flights' staying time in the cargo hangar. The objective function minimizes the overall penalty costs in supporting mission flight's operations, including the penalties of rejecting arrival of mission aircraft during the planning period, late departure of mission aircraft and failing to dispatch mission flights at the end of planning period.

$s.t.$

The constraints involved in the proposed mathematical model are divided into several sections for easy presentation and descriptions:

1) Mission aircraft's landing and departure sequencing and scheduling on runway

The arrangement of the landing and departure time for the incoming mission aircraft is subjected to the runway capacity. In addition, the assigned landing and departure time must be larger than the minimum separation time between two consecutive aircraft, which is determined by the aircraft's classes and the operation mode of the current runway.

$$Arrt_i - Arrt_j \geq s_{ij} - M(1 - sqrAA_{jir}), \forall i, j \in A_T, \forall r \in R \quad (1)$$

$$rwyL_{ir} + rwyL_{jr} \leq 1 + sqrLL_{ijr} + sqrLL_{jir}, \forall i, j \in A_T, \forall r \in R \quad (2)$$

$$sqrLL_{jir} + sqrLL_{ijr} \leq 1, \forall i, j \in A_T, \forall r \in R \quad (3)$$

$$Dept_i - Dept_j \geq s_{ij} - M(1 - sqrDD_{jir}), \forall i, j \in A_T, \forall r \in R \quad (4)$$

$$rwyD_{ir} + rwyD_{jr} \leq 1 + sqrDD_{ijr} + sqrDD_{jir}, \forall i, j \in A_T, \forall r \in R \quad (5)$$

$$sqrDD_{jir} + sqrDD_{ijr} \leq 1, \forall i, j \in A_T, \forall r \in R \quad (6)$$

$$Arrt_i - Dept_j \geq s_{ij} - M(1 - sqrDA_{jir}), \forall i, j \in A_T, \forall r \in R \quad (7)$$

$$rwyL_{ir} + rwyD_{jr} \leq 1 + sqrDA_{ijr} + sqrDA_{jir}, \forall i, j \in A_T, \forall r \in R \quad (8)$$

$$sqrDA_{jir} + sqrDA_{ijr} \leq 1, \forall i, j \in A_T, \forall r \in R \tag{9}$$

$$Dept_i - Arrt_j \geq s_{ij} - M(1 - sqrAD_{jir}), \forall i, j \in A_T, \forall r \in R \tag{10}$$

$$rwyD_{ir} + rwyL_{jr} \leq 1 + sqrAD_{ijr} + sqrAD_{jir}, \forall i, j \in A_T, \forall r \in R \tag{11}$$

$$sqrAD_{jir} + sqrAD_{ijr} \leq 1, \forall i, j \in A_T, \forall r \in R \tag{12}$$

$$Arrt_{ir} \geq TGAT_i, \forall i \in A_T, \forall r \in R \tag{13}$$

$$Dept_{ir} - Arrt_{ir} \geq CPT_i, \forall i \in A_T, \forall r \in R \tag{14}$$

$$\sum_{t \geq tg\_at_i} rollin_{it} \cdot t \geq Arrt_{ir}, \forall i \in A_T, \forall r \in R \tag{15}$$

$$Dept_{ir} \geq \sum_{t \geq tg\_at_i} rollout_{it} \cdot t, \forall i \in A_T, \forall r \in R \tag{16}$$

$$\sum_{r \in RWY} rwyA_{ir} \leq 1 - RJF_i, \forall i \in A_T, \forall r \in R \tag{17}$$

$$\sum_{r \in RWY} rwyD_{ir} \leq 1 - RJF_i, \forall i \in A_T, \forall r \in R \tag{18}$$

$$\sum_{r \in RWY} rwyA_{ir} \geq 1 - RJF_i, \forall i \in A_T, \forall r \in R \tag{19}$$

$$\sum_{r \in RWY} rwyD_{ir} \geq 1 - RJF_i, \forall i \in A_T, \forall r \in R \tag{20}$$

$$\sum_{r \in RWY} rwyD_{ir} \leq 1 - MDF_i, \forall i \in A_T, \forall r \in R \tag{21}$$

$$\sum_{r \in RWY} rwyD_{ir} \geq 1 - MDF_i, \forall i \in A_T, \forall r \in R \tag{22}$$

$$MDF_i = rollout_i^*, \forall i \in A_T, \forall r \in R \tag{23}$$

$$rwyA_{ir} \in \{0,1\}\ \forall i \in A_T, \forall r \in R \tag{24}$$

$$sqrA_{ijr} \in \{0,1\}\ \forall i \in A_T, \forall r \in R \tag{25}$$

$$rwyD_{ir} \in \{0,1\}\ \forall i \in A_T, \forall r \in R \tag{26}$$

$$sqrD_{ijr} \in \{0,1\}\ \forall i \in A_T, \forall r \in R \tag{27}$$

$$RJF_i \in \{0,1\}, \forall i \in A_T \tag{28}$$

$$MDF_i \in \{0,1\}\ \forall i \in A_T \tag{29}$$

$$Arrt_{ir} \geq 0, \forall i \in A_T, \forall r \in R \tag{30}$$

$$Dept_{ir} \geq 0, \forall i \in A_T, \forall r \in R \tag{31}$$

The landing/take-off separation and mission flight sequencing constraints are divided into four scenarios according to the relations between two mission flights, namely departure-departure, landing-departure, departure-landing and landing-landing scenarios.

Taking landing-landing scenario as an example to illustrate the constraint set; Constraint (1) computes the assigned landing time for each flight *i*, and imposes the separation time of landing operations between aircraft *i* and the preceding landing aircraft *j* on the same runway. Constraints (2) and (3) determine the sequence between two aircraft using the same runway for landing operations, prescribing that $sqrLL_{ijr}$ equals to 1 if flight *i* lands on runway *r* after the arrival of flight *j* (not necessarily immediately) and 0 if otherwise. The same logic apply to Constraints (4) – (6), (7)-(9) and (10)-(12) for departure-departure scenario, landing-departure scenario, departure-landing scenario, respectively.

Constraint (13) prescribes that the landing time of the mission aircraft must be equal to or larger than the target arrival time. Constraint (14) makes sure that mission aircraft's staying duration at the airport should be equal to or longer than the required cargo handling time, so as to conduct the cargo loading/off-loading tasks. Constraint (15) prescribes that rolling in time to cargo hangar should be equal to or later than mission aircraft's landing time on airport runway, and Constraint (16) restricts that mission aircraft can conduct take-off operations only after it has completed cargo handling task and rolled out from the cargo hangar. Constraints (17) and (18) restrict mission aircraft *i* to using only one runway for landing and departure operations. Constraints (19) and (20) restrict that the landing and departure operations cannot be conducted if the mission aircraft is rejected by the airport. Constraint (21) prescribes that the departure operations cannot be conducted if mission aircraft's cargo handing task are not completed by the end of planning horizon, and Constraint (22) connects the relevant decision variables from aircraft sequencing and hangar planning components in the mathematical model. Constraint (23) prescribes that the rolling in operations cannot be conducted if the mission aircraft is rejected by the airport. Constraints (24) – (29) indicate the binary variables in the mathematical model. Constraints (30) – (31) ensure that the coordinates of the aircraft are positive.

2) Non-overlapping constraint in the cargo processing hangar

Regarding the aircraft parking arrangement in the cargo hangar during the entire planning period, the planning timeline is composed of multiple discrete event time point scattered along the whole period (as shown in Figure 5). Each time point *t* records the position of aircraft in the hangar and their movement operations.

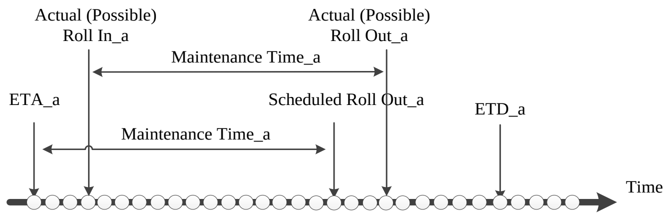

Figure 5 Basic discrete-time model

The mission aircraft's cargo loading and unloading task should only be done in a cargo processing hangar. Therefore, the parking position of aircraft should be within the boundary of the cargo hangar, observing a minimum safety margin with the other aircraft parked in the hangar. The No-Fit Polygons introduced in Section 3.2 are converted to non-overlapping constraints for all incoming mission aircraft.

$$x_i + wa_i / 2 \le WH, \ \forall i \in A_T \tag{32}$$

$$x_i \ge wa_i / 2, \ \forall i \in A_T \tag{33}$$

$$y_i + la_i \le LH, \ \forall i \in A_T \tag{34}$$

$$\alpha_{ij}^{kf}(x_j - x_i) + \beta_{ij}^{kf}(x_j - x_i) \le q_{ij}^{kf} + M \cdot (1 - b_{ijkt}), \ \forall i, j \in A_t, \ \forall k = 1, 2, ..., m_{ij}, \ \forall f = 1, 2, ..., t_{ij}^{k}, , \forall t \ge 0 \tag{35}$$

$$\sum_{k=1}^{m_{ij}} b_{ijkt} \le p_{it}, \ \forall i, j \in A_t, \forall t \ge 0 \tag{36}$$

$$\sum_{k=1}^{m_{ij}} b_{ijkt} \le p_{jt}, \ \forall i, j \in A_t, \forall t \ge 0 \tag{37}$$

$$\sum_{k=1}^{m_{ij}} b_{ijkt} \le 1 - rollout_{it}, \ \forall i \in D_t, \forall t \ge 0 \tag{38}$$

$$\sum_{k=1}^{m_{ij}} b_{ijkt} \le 1 - rollout_{jt}, \ \forall j \in D_t, \forall t \ge 0 \tag{39}$$

$$\sum_{k=1}^{m_{ij}} b_{ijkt} \ge p_{it} + p_{jt} - 1, \ \forall i, j \in A_t \backslash D_t, \forall t \ge 0 \tag{40}$$

$$\sum_{k=1}^{m_{ij}} b_{ijkt} \ge p_{it} + p_{jt} - (rollout_{it} + rollout_{jt}) - 1, \ \forall i, j \in D_t, \forall t \ge 0 \tag{41}$$

$$\sum_{k=1}^{m_{ij}} b_{ijkt} \ge p_{it} + p_{jt} - rollout_{it} - 1, \ \forall i \in D_t, \forall j \in A_t \setminus D_t, \forall t \ge 0 \tag{42}$$

$$\sum_{k=1}^{m_{ij}} b_{ijkt} \ge p_{it} + p_{jt} - rollout_{jt} - 1, \ \forall i \in A_t \setminus D_t, \forall j \in D_t, \forall t \ge 0 \tag{43}$$

The boundary constraint is imposed by Constraints (32)-(34), which ensure that the incoming mission aircraft park within the cargo hangar. Specifically, Constraints (32) and (33) impose that the left wing and right wing of an aircraft are within the boundary of hangar, from x-axis direction. Constraint (34) imposes that the head of an aircraft is within the boundary of hangar, from y-axis direction. The geometrical information of No-Fit Polygons is expressed in Constraint (35), and Constraints (36) – (43) control the activation of non-overlapping constraint. Specifically, Constraint (35) is activated by Constraint (40) at time *t* under the condition that both two aircraft are staying in or moving into cargo hangar. The non-overlapping constraint becomes inactive if any one of them is not staying in the cargo hangar, or one of them is moving out from hangar at the same time *t*. Decision variable p_{it} denotes whether aircraft *i* is staying in hangar at time *t*. Binary variable b_{ijkt} imposes the position of aircraft *j*'s coordinates, which is associated with the horizontal slice *k* outside the *NFP* between aircraft *i* and *j*.

3) Aircraft movement blocking restriction constraints

Mission aircraft's movement operations should not be blocked by any other aircraft staying in the cargo hangar, otherwise the movement operations will have to be postponed or suspended until the movement path to the target parking position or hangar exit becomes clear. The blocking restriction relation is denoted by the auxiliary variables h_{ijt}, L_{ij}, R_{ij} and U_{ij}.

$$(x_i + wa_i/2) - (x_j - wa_i/2) \le M \cdot (1 - L_{ij}) \quad \forall i \in A_t, \forall j \in A_t \setminus i, \forall t \ge 0 \tag{44}$$

$$(x_i - wa_i/2) - (x_j + wa_i/2) \ge -M \cdot (1 - R_{ij}) \quad \forall i \in A_t, \forall j \in A_t \setminus i, \forall t \ge 0 \tag{45}$$

$$(y_i + TailD_i) - (y_j + TailD_j) \ge -M \cdot (1 - U_{ij}) \quad \forall i \in A_t, \forall j \in A_t \setminus i, \forall t \ge 0 \tag{46}$$

$$(1 - h_{ijt}) \ge \frac{1}{6} \cdot \left[L_{ij} + R_{ij} + U_{ij} + rollin_{jt} + rollout_{jt} + (1 - p_{jt}) \right] \quad \forall i \in A_t, \forall j \in D_t, \forall t \ge 0 \tag{47}$$

$$(1 - h_{ijt}) \le L_{ij} + R_{ij} + U_{ij} + rollin_{jt} + rollout_{jt} + (1 - p_{jt}) \quad \forall i \in A_t, \forall j \in D_t, \forall t \ge 0 \tag{48}$$

$$(1 - h_{ijt}) \ge \frac{1}{5} \cdot \left[L_{ij} + R_{ij} + U_{ij} + rollin_{jt} + (1 - p_{jt}) \right] \quad \forall i \in A_t, \forall j \in A_t \setminus D_t, \forall t \ge 0 \tag{49}$$

$$(1 - h_{ijt}) \le L_{ij} + R_{ij} + U_{ij} + rollin_{jt} + (1 - p_{jt}) \quad \forall i \in A_t, \forall j \in A_t \setminus D_t, \forall t \ge 0 \tag{50}$$

$$rollout_{it} \le 1 - \frac{1}{|A_t \setminus i|} \cdot \sum_{\forall j \in A_t \setminus i} h_{ijt}, \forall i \in D_t, \forall t \ge 0 \tag{51}$$

$$rollin_{it} \le 1 - \frac{1}{|A_t \setminus i|} \cdot \sum_{\forall j \in A_t \setminus i} h_{ijt}, \forall i \in A_t, \forall t \ge 0 \tag{52}$$

Constraints (44) – (46) determine and impose the relative position relations between aircraft. Specifically, binary variables L_{ij}, R_{ij} and U_{ij} with value of 1 indicates that aircraft *i* is on the left, right, or above aircraft *j* respectively, and is not blocking the movement operations for aircraft *i*. Furthermore, the consolidated binary variable h_{ijt} reflects the overall relation between aircraft *i* and *j*, and the value of h_{ijt} is controlled by Constraints (47) – (50). In addition, if aircraft *j* is undertaking movement operations at the same time as aircraft *i*, the above-mentioned blocking restriction constraints are relaxed. Constraints (51) and (52) indicate that the movement operations for mission aircraft cannot commence if the blocking indicating variable h_{ijt} returns a negative feedback on the relative position relation between aircraft *i* and the other aircraft in the hangar.

4) Cargo loading and unloading processing time constraint

Mission aircraft's staying time in the cargo hangar should be sufficient for completing the cargo processing task, and the relevant constraints are developed in this subsection.

$$(\sum_{t\geq ETD_i} rollout_{it}\cdot t - \sum_{t\geq ETA_i} rollin_{it}\cdot t) + M\cdot(1-\sum_{t\geq ETA_i} rollin_{it}) + M\cdot(1-\sum_{t\geq ETD_i} rollout_{it}) \geq CPT_i, \forall i\in A_T \quad (53)$$

$$p_{it} = \sum_{ETA_i\leq m\leq t} rollin_{im}, \forall i\in A_T, \forall ETA_i \leq t\leq ETD_i \quad (54)$$

$$p_{it} = \sum_{ETA_i\leq m\leq t} rollin_{im} - \sum_{ETD_i\leq m\leq t-1} rollout_{im}, \forall i\in A_T, \forall t\geq ETD_i+1 \quad (55)$$

$$\sum_{t\geq ETA_i} rollin_{it} \leq 1, \forall i\in A_T \quad (56)$$

$$\sum_{t\geq ETD_i} rollout_{it} \leq 1, \forall i\in A_T \quad (57)$$

$$rollout_{it} \leq \sum_{ETA_i\leq m< t} rollin_{im}, \forall i\in A_T, \forall t\geq ETD_i \quad (58)$$

$$(1-rollout_{iT*}) \leq \sum_{t\geq ETD_i} rollout_{it} + M\cdot(1-\sum_{t\geq ETA_i} rollin_{it}), \forall i\in A_T \quad (59)$$

Constraint (53) imposes that the staying time of mission aircraft in the cargo processing hangar should be equal to or longer than the associated cargo loading/unloading time, given that the mission flight is accepted by the airport. Constraints (54) – (55) determine the value of binary variable p_{it}, which indicates whether aircraft *i* is staying in cargo hangar at time *t*. If the value of p_{it} equals to one, the corresponding non-overlapping constraints mentioned above are activated to prevent aircraft *i* from overlapping with other aircraft in the hangar. Constraints (56) – (58) ensure the logics of moving in and moving out operations of each mission aircraft. Constraint (59) determines the value of binary variable out_{iT^*}, which indicates whether aircraft *i* can be dispatched from the airport at the end of the planning period.

5) Geometrical-related decision variables range constraints

$$x_i, y_i \geq 0 \quad \forall i\in A_T \quad (60)$$

$$b_{ijkt} \in \{0,1\} \ \forall i,j\in A_t, k=1,2,...,m_{ij}, \forall t\geq 0 \quad (61)$$

$$p_{it} \in \{0,1\} \quad \forall i \in A_t, \forall t \geq 0 \tag{62}$$

$$rollin_{it} \in \{0,1\}, \forall i \in A_t, \forall t \geq 0 \tag{63}$$

$$rollout_{it} \in \{0,1\}, \forall i \in D_t, \forall t \geq 0 \tag{64}$$

$$rollout_{iT*} \in \{0,1\}, \forall i \in D_t, \forall t \geq 0 \tag{65}$$

$$h_{ijt}, L_{ij}, R_{ij}, U_{ij} \in \{0,1\} \quad \forall i \in A_t, \forall j \in A_t \setminus i, \forall t \geq 0 \tag{66}$$

Constraint (60) ensures that the coordinates of the aircraft are non-negative, and Constraints (61) – (66) indicate the binary variables in the mathematical model.

4. Development of a Two-stage Optimization Method

The mathematical model developed in Section 3 becomes intractable in resolving large-scale problem instances, given a large number of discrete time points associated with geometrical-related decision variables and runway sequencing and scheduling decision variables. In this section, we present a two-stage optimization method to enhance the efficiency in searching for high quality solutions. Considering the complexity in simultaneously optimizing runway and hangar resources, we introduce an optimization algorithm to speed up the optimization process while maintaining high solution quality.

The original model proposed in Section 3 integrates the decision variables and constraints related to aircraft's arrival and departure sequencing and scheduling on runway, and aircraft's movement operations in cargo hangar, which describes the interdependent relations between these two major decision-making components. In the integrated model, updating bounds or identifying better incumbent solutions with conventional branch-and-bound algorithm becomes challenging as the default branching strategy is not able to comprehend the hierarchal structure of decision-makings and practical meanings of the proposed model.

The appropriate flow of the decision-making sequence should be: 1) determining the landing runway and landing time for each incoming mission aircraft; 2) arranging arrival mission aircraft's parking position and roll-in/roll-out time (cargo processing time window) to cargo hangar and 3) determining the departure runway and take-off time. The respective constraint sets are imposed on the respective decision-making stages accordingly, including the separation time constraints for aircraft landing and departure; non-overlapping constraints and movement blocking constraints for aircraft parking and movement arrangements in the cargo hangar.

To alleviate computational difficulties, the optimization mechanism is reorganized in a two-stage optimization approach, as shown in Figure 6. Firstly, we ignore possible movement blockages and delays that may occur in the cargo hangar, and determine the mission aircraft's landing and take-off sequence and schedule with respective standard turnaround time (the normal cargo handling time associated with each mission aircraft). Afterwards, the aircraft's landing and take-off schedule is validated by the constraints associated with cargo hangar arrangement, including constraints associated with NFP to prevent aircraft overlapping and constraints describing movement blocking. If incoordinate feedback returns, aircraft's runway sequence, schedule and turnaround time window should be adjusted iteratively. As the original model is decomposed into two subproblems in the two-stage optimization approach, the linkage between runway scheduling and cargo hangar layout planning is weakened. Therefore, the optimality gap of the original problem cannot be explicitly obtained. Nevertheless, when solving medium- and large-scale instances, the default branch-and-bound algorithm is incapable to obtain a feasible solution for the original problem. In this regard, a trade-off between computational performance and optimality indication is achieved by the proposed two-stage optimization approach.

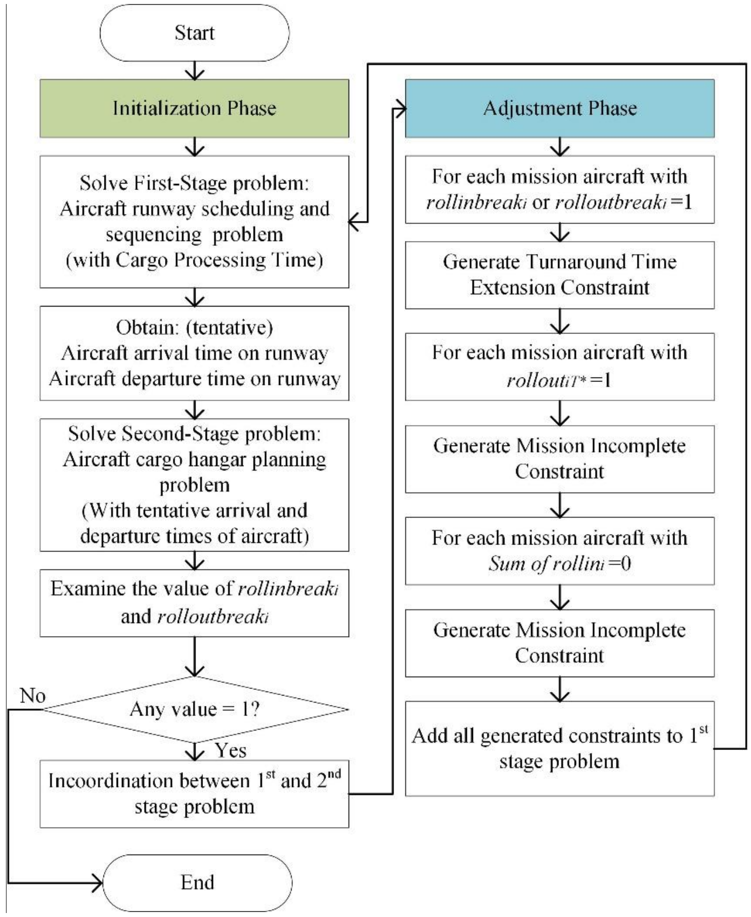

Figure 6 Algorithmic framework of the two-stage optimization method

4.1 First-stage problem: Aircraft arrival and departure sequencing and scheduling on runway

Subject to runway capacity and the consideration of separation time between two consecutive landing/take-off operations on the same runway, the mission aircraft's landing and take-off sequences and time are optimized in this section, without taking the limit of cargo hangar capacity into consideration. The constraints involved in the aircraft sequencing and scheduling model are the separation time constraint for two consecutive flights on the same runway, and the cargo loading/unloading processing time (i.e., mission flights' turnaround time at the airport). It is assumed that the cargo processing time is longer than the aircraft turnaround time, which will be absorbed by the cargo processing time. As the planning horizon starts from the earliest target arrival time of the mission aircraft, it ends at the latest (target arrival time + cargo processing time) or the latest target departure time of the mission aircraft. Under traffic congestion scenarios, runway and cargo resources are insufficient to accommodate all mission aircraft. Therefore, it is possible that some aircraft cannot depart punctually, and will have to stay at the cargo hangar till the end of planning horizon. Under such circumstances, penalty costs (penalty3 in the mathematical model notation) for those aircraft that fail to complete their cargo transportation mission are incurred. The optimized solution obtained in this section satisfies the minimum turnaround time constraints. Then, the corresponding landing/departure schedules become parameters and are passed to the aircraft parking position arrangement problem at the second stage. Specifically, the optimized landing and take-off time for the mission aircraft are considered as the expected arrival and departure time at the second-stage.

The aircraft runway sequencing and scheduling problem in this stage is optimized by the MILP model, which is derived from constraints (1) – (31) in the model proposed in Section 3.3. The objective function of the first-stage problem minimizes the tardiness of mission aircraft departure and the mission flight rejection penalties.

At the very beginning of optimization in this stage, the turnaround time for each mission aircraft equals to the input cargo handling time, assuming that all mission aircraft can complete their respective cargo loading/unloading task timely. In other words, each incoming mission aircraft's cargo processing/moving operations are not delayed in the cargo hangar. As the iteration process continues, the aircraft landing and take-off schedule determined in the first-stage of the problem may be incompatible with the cargo hangar accommodating capability as the number of incoming aircraft grows. Therefore, aircraft's landing and take-off schedule needs to be adjusted in the first-stage of optimization at the next iteration. As long as the take-off time schedule matches the aircraft movement operations and cargo processing task in the cargo hangar in the second stage, the adjustment on runway sequencing and scheduling will be terminated.

4.2 Second-stage problem: aircraft parking and movement planning in cargo hangar

The delays of mission aircraft' movements in the cargo hangar are common when the hangar needs to accommodates many aircraft during peak hours. Under such circumstances, mission aircraft's movement operation may be blocked, leading to some aircraft not being able to conduct their cargo handling tasks according to the planned turnaround time window determined during the first-stage problem. Therefore, tardiness in movement operations and aircraft's departure time can occur. To resolve the discrepancy between the two stage decisions made, the landing/take-off schedule and turnaround time have to be adjusted to align with the cargo accommodating capability.

The aircraft's cargo hangar arrangement problem at the second stage is derived from constraints (32) – (65) in the model proposed in Section 3.3, in addition to the mission aircraft's planned landing and departure time obtained from the first-stage problem. Specifically, the aircraft landing and take-off schedules obtained from the first-stage are converted to parameters in the second-stage problem, which validates the feasibility of the time window. There are two possible optimization outcomes during the second-stage optimization. 1) If aircraft's roll in and roll out time returned from the second-stage problem exceed the landing and take-off time windows determined in the first-stage problem under the current iteration, the roll in and roll out time obtained from the second-stage problem forms a revised turnaround time duration constraint, which is imposed to the first-stage problem at the next iteration. 2) A feasible solution returns after optimizing the second-stage problem, which implies that all mission aircraft's cargo handling task can be completed within the landing and take-off time windows determined in the first-stage problem. Aircraft's landing and take-off time adjustment is not necessary, and therefore a feasible solution corresponding to the original problem is obtained.

To determine if the second-stage problem's roll in and roll out time exceed the landing and take-off time windows determined in the first-stage problem, the following auxiliary binary decision variables are introduced to form the second-stage problem model.

$rollin\_break_i$	1, if mission aircraft *i*'s roll in time into cargo hangar is not equal to the assigned landing time obtained from the first-stage problem, and 0 otherwise
$rollout\_break_i$	1, if mission aircraft *i*'s roll out time from cargo hangar is later than assigned take-off time obtained from the first-stage problem, and 0 otherwise

The assigned mission aircraft's landing and take-off time associated with respective runways obtained from the first-stage problem become parameters under this stage. Ideally, all mission aircraft's roll in and roll out time are within each aircraft's landing and take-off time windows, which means that cargo handling tasks do not induce any tardiness to the mission aircraft's flight schedule. Nevertheless, aircraft's landing and take-off time can be adjusted if cargo hangar's capability cannot timely process all incoming mission flights' cargo loading and unloading needs. The following constraints are introduced to indicate whether an aircraft's roll in and roll out time exceed the time windows of the assigned landing and take-off time determined in the first-stage problem.

$$rollin_{it} \geq 1 - rollinbreak_i, t = \overline{ALT}_i \tag{67}$$

$$rollout_{it} \geq 1 - rolloutbreak_i, t = \overline{ADT}_i \tag{68}$$

Constraints (67) and (68) indicate that mission aircraft's cargo hangar roll in and roll out time can break the time window of landing and take-off determined in the first-stage problem. The values of $rollin\_break_i$ and $rollin\_break_i$ equal to 1 if the aircraft's roll in time and roll out time are beyond the landing and take-off time derived from the first-stage problem, respectively. It implies that the time gap between landing and take-off time is not sufficient for processing cargo in the hangar. In the next iteration, aircraft's staying time in the cargo hangar will be extended, resulting in a longer time gap between the landing and take-off time in the first-stage problem.

4.3 Optimization iteration between the first-stage and second-stage problem

If aircraft's roll in and roll out time fall outside of the landing and take-off time windows, incoordination of local decisions between the first-stage problem and the second-stage problem occurs. Given that the cargo processing hangar's accommodating capacity is limited and cannot be expanded during the planning period, the possible alternatives to eliminate the incoordination between two stages include extension of landing and take-off time window duration by postponing the planned take-off time, rejection of the mission aircraft that cannot be accommodated during the planning period, and delaying the mission aircraft's departure during the planning period.

The relevant constraints for implementing the above-mentioned alternatives are listed as follows:

To extend aircraft's landing and take-off time window, the roll in and roll out time determined in the second-stage problem provide a reference of lower bound for the minimum turnaround time.

$$Dept_i - Arrt_i \geq (\sum_{t \geq ETD_i} \overline{rollout}_{it} \cdot t - \sum_{t \geq ETA_i} \overline{rollin}_{it} \cdot t), \forall i \in \overline{rollinbreak_i} = 1 \cup \overline{rolloutbreak_i} = 1 \quad (69)$$

Constraint (69) extends the landing and take-off time window duration, which is added to the first-stage problem to adjust aircraft sequence and schedule on the runway. The length of turnaround time extension is calculated based on the roll in and roll out time derived from the second-stage problem.

Mission flight's rejection decision is indicated by the roll in rejection determined in the second-stage problem.

$$RJF_i = 1, \{ i \mid \sum_{t \geq Arrt_i} rollin_{it} = 0 \} \quad (70)$$

Mission flight's delay departure decision under the current planning period is indicated by the roll out delay decision determined in the second-stage problem.

$$MDF_i = 1, \{ i | rollout_i^* = 1 \} \; \forall i \in A_T \quad (71)$$

Adoption of local decision coordination alternatives is objective-value-oriented. The expected tardiness cost caused by adjusting the landing and take-off time are evaluated, and the adjusted schedule with minimal penalty cost is identified as a reference solution for the next iteration.

Algorithm 1

Two-stage optimization approach for runway scheduling and aircraft parking planning

Notations	Meanings
ALT_i, ADT_i	Assigned landing time and take-off time for mission aircraft i, determined by the first stage problem
$ARIT_i, AROT_i$	Assigned roll in time and roll out time for mission aircraft i, determined by the second stage problem
A_T	All incoming mission flights during the planning period
$rollinbreak_i$	Indicator of breaking the assigned landing time of flight i at the second stage problem
$rolloutbreak_i$	Indicator of breaking the assigned take-off time of flight i at the second stage problem
$rollout_i^*$	Indicator of delay departure of mission flight i at the second stage problem

1: Initialization phase: Determine the landing time, take-off time and operations sequence on runways for all incoming mission aircraft by solving the first-stage problem, with original cargo handling time. Go to Step 3.

2: Adjustment phase: Adjust the landing time, take-off time and operations sequence for all incoming mission aircraft with the feedback from the second stage problem, with the reference information and constraints associated with cargo roll in and roll out time.

3: Determine mission aircraft's cargo hangar roll in and roll out time, according to the assigned landing and take-off time derived from the first-stage problem.

4: If the value of $rollinbreak_i$ or $rolloutbreak_i$ equals to one, the incoordination between aircraft landing-take-off cycle and cargo hangar arrangement occurs.

5: Review incoordination elimination alternatives through the indicating binary variables

6: For *i* in A_T

7: If $rolloutbreak_i = 1$ or $rollinbreak_i = 1$

8: Generate turnaround time extension constraint $Dept_i - Arrt_i \geq (\sum_{t \geq ETD_i} \overline{rollout_{it}} \cdot t - \sum_{t \geq ETA_i} \overline{rollin_{it}} \cdot t)$ for the associated aircraft and add the constraint to the first-stage problem.

9: If $RollOutT*_i = 1$

10: Generate the $MDF_i \geq 1, \{i | rollout_i^* = 1\}$ constraint. Add the constraint to the first stage problem

11: If $\sum_{t \geq ALT_i} rollin_{it} = 0$

12: Generate the $RJF_i \geq 1, \{i \mid \sum_{t \geq Arrt_i} rollin_{it} = 0\}$ constraint. Add the constraint to the first stage problem
13: Go to Step 2 (Adjustment phase).
14: Else if the second stage solution is feasible
15: The current local solutions of both two stage problems are aligned with each other. A feasible solution corresponding to the original problem can be obtained. Go to Step 16.
16: End

4.4 Enhancement of second-stage problem MILP model

Although the two-stage optimization approach alleviates the computational difficulties in solving the original MILP model, there are a large number of discrete time points involved in the second-stage problem. To describe the status and solution of each discrete time point, the values of geometrical decision variables (x_i , y_i , h_{ijt} , L_{ij} , R_{ij} , U_{ij} , p_{it} , in_{it} and out_{it}) represent the geometrical relations under current time *t*. The computational complexity of the second-stage problem grows significantly as the planning period is lengthened and the interval between time points is reduced. To avoid visiting large numbers of unpromising discrete time points that are not likely to trigger any movement operations, a possible-movement discrete time identification method is proposed to further tighten the MILP model of the second-stage problem. The main idea is eliminating all unpromising time points and keeping those discrete time points that may trigger movement operations.

Based on the First-Come-First-Served and Roll-Out-Upon-Finishing practices, the possible movement time consist of basic possible movement timings and delayed movement timings when blockage in the cargo hangar occurs. The basic possible movement timings refer to mission aircraft's roll in and roll out time without any blockage in the hangar. Therefore, the basic possible roll in time equals to the assigned landing time $Arrt_i$ determined in the first-stage problem, and the basic possible roll out time equals to the assigned landing time in addition to the standard cargo handling time ($Arrt_i + CHT_i$). Under practical scenarios, there are multiple mission aircraft in the cargo hangar conducting cargo processing tasks concurrently, and it is common that their movement operations cannot be conducted timely if congestion occurs during peak hours. Therefore, some mission aircraft's movement operations are delayed even though their cargo processing tasks have been completed, and their respective movement operations can only be conducted after the other mission aircraft blocking its movement paths have left the cargo hangar. The delayed movement timings can be derived by recursively calculating each incoming mission aircraft's possible movement time, according to the First-Come-First-Serve practice.

Example. There are three incoming mission aircraft, associated with their assigned landing times $Arrt_1$, $Arrt_2, Arrt_3$ determined in the first-stage problem, where $Arrt_1 < Arrt_2 < Arrt_3$. The cargo handling time for the three mission aircraft are CHT_1, CHT_2, CHT_3, where $CHT_1 < CHT_2$. If the cargo hangar's space is limited, mission aircraft 2 may need to wait for mission aircraft 1 to complete its cargo handling task and leave the hangar, then the corresponding possible roll in time of mission aircraft 2 is $Arrt_1 + CHT_1$. Another situation demonstrates the chain effect of movement blocking and the impact of later arrival aircraft have on aircraft already parked in cargo hangar. Specifically, if the later arrival mission aircraft 3 has a relatively long cargo handling time, mission aircraft 1 and 2's roll out path may be blocked by aircraft 3. Then, aircraft 1 and 2's possible roll in time will become $Arrt_3 + CHT_3$, $Arrt_3 + CHT_3$, respectively,

The recursive calculation of possible movement time for the second stage MILP model is described in **Algorithm 2**.

Algorithm 2 Possible movement timing for the second stage MILP model

Notations	Explanations
A_T	All incoming mission flights during the planning period
$Possible\_RollIn_i$	Set of possible moving-in operation time for mission aircraft *i*
$Possible\_RollOut_i$	Set of possible moving-out time for mission aircraft *i*
SEQ	The sequence of all mission flights sorted by respective assigned landing time
Seq_n	The mission aircraft with sequence *n*

1: List all mission flights according to their assigned landing time ALT_i in increasing order, then derive the sequence of flights and record as Seq_n.

2: $n = 1, 2, 3, \ldots, N$ Seq_n

(Computation of possible moving-in time)

for $n = 1, 2, 3, \ldots, N$ in Seq_n

3: for $1 < n^{'} < n$

4: If $Possible\_MoveIn_{n'} + CHT_{n'} > ALT_n$

5: Include $Possible\_MoveIn_{n'} + CHT_{n'}$ into $Possible\_MoveIn_n$

(Computation of possible moving-out time)

6: for $n = 1, 2, 3, \ldots, N$ in Seq_n

7: Include $ALT_n + CPT_n$ into $Possible\_MoveOut_n$

8: Include all $Possible\_MoveIn_n + CPT_n$ into $Possible\_MoveOut_n$

(Chain effect on the possible moving-out time brought by the subsequent mission aircraft)

9: for $n^{'} > n$ (if $n \neq N$)

10: If $ALT_{n'} \geq Possible\_MoveIn_n$

11: For $Possible\_MoveIn_{n'}$

12: If $Possible\_MoveIn_{n'} + CHT_{n'} \geq Possible\_MoveIn_{n'} + CHT_{n'}$

13: Include $Possible\_MoveIn_{n'} + CPT_{n'}$ into $Possible\_RollOut_n$

5. Computational experiments

To examine the performance of the proposed optimization approach in resolving practical problems, we performed several computational experiments with different parameters and problem instances settings. All procedures of the mathematical model and algorithms described in Sections 3 and 4 were coded in C# in Visual Studio Community 2019 and run on a computer with an Intel Core i7-9700 processor, at 3.00 GHz with 32 Gb of RAM. The Mixed-Integer Linear Programming model described in Section 3 was solved by the CPLEX 12.7.0.0 serial model [53].

5.1 Description of test instances

Problem instances are created according to real situations under post-disaster relief scenarios, which include 23 types of mission aircraft. The expected landing time, expected departure time as well as the cargo handling time for each mission flight are included in the instance. Referring to the instance setting methods in [33], the patterns of mission aircraft arrivals under normal and traffic congestion situations were created in order to examine the efficiency and solution quality of the proposed optimization method. Regarding the duration of planning horizon, it is determined by the specification of mission aircraft involved in the instances. In particular, the planning horizon starts from the earliest target arrival time of mission aircraft and ends at the latest (target arrival time + cargo processing time) or the latest target departure time of mission aircraft. A detailed information regarding the geometrical information of the mission aircraft is listed in Table 1. The arriving pattern and the cargo handling complexity (handling lead time) are presented in Table 2. The separation time between two consecutive aircraft on the same runway are prescribed according to aircraft types. In particular, the separation time for consecutive flights on the same runway is presented in Table 2. As we only consider flights for cargo transportation mission, the overall congestion level is evaluated by integrating the situations on the runway and cargo hangar operations, and the classification of the traffic congestion level is presented in Table 3.

Table 1 Geometrical information of mission type

Aircraft Type	Length (meters)	Width (meters)
G200	19	18
CL600	21	19
CL605	21	20
F900LX	20.2	21.4
F2000EX	20.3	21.4
F2000LX	20.3	21.4
ERJ135	27	20
F7X	24.3	26.4
G450	27.2	23.6
GIV	27	24
GL5T	29	29
G550	29.4	28.6
G5000	29.5	28.6

G6000	30.4	30.4
G650	31	31
A318	31.5	34.2
ERJ190	36.4	29
A319	34	36
A320	37.6	36
B738	39.6	38
A321	44.6	36
A332	58.4	60.3
A333	63.7	60.3

Table 2 Runway separation time for consecutive flights

Aircraft types	Small-sized aircraft	Medium-sized aircraft & Large-sized aircraft
Small-sized aircraft	3 minutes	4 minutes
Medium-sized aircraft & Large-sized aircraft	4 minutes	4 minutes

Table 3 The classification of traffic congestion level and the description of mission aircraft's arrival pattern

Congestion Level	Number of arrival mission flights	Average Cargo handling time (hours)
Normal – Level 1	3-5	24
Light arrival congestion – Level 2	6-8	35
Moderate arrival congestion – Level 3	9-10	40

5.2 Computational experiment

Two sets of computational experiments were performed, examining the efficiency and solution quality of the original discrete-time mathematical model developed in Section 3 and the proposed two-stage optimization method proposed in Section 4. Section 5.2.1 compares the performances of the original discrete-time model with different time interval settings along the planning period. Section 5.2.2 compares the two-stage optimization methods with and without the second-stage problem model enhancement methods proposed in Section 4.4.

5.2.1 Evaluation of mathematical models

Considering that the time interval between two consecutive time points is one of the major determinants of model complexity, we compared the solution efficiency and quality by adopting different time interval settings while solving small- and medium-scale problem instances. Tables 3 and 4 present the results of solving 29 problem instances with different time interval settings. Although setting a short time interval enhances the accuracy of the solution, the problem complexity increases significantly as large number of redundant discrete time points hinder the branch-and-bound progress. To maintain a tradeoff between model complexity and accuracy, the time intervals were prescribed as 30 minutes, 60 minutes, 120 minutes and 300 minutes. Instance names are listed in the first column of Tables 3 and 4. The format of instance name is set as "congestion level_number of incoming mission aircraft (serial number)", where the serial number is used to differentiate the instances with the same number of incoming mission flights and planning days. For example, 2_7(4) represents a problem instance involving 7 arrival mission flights (the 4^{th} instance with 7 mission flights). Each instance was solved by using the original mathematical model with 4 discrete time interval settings, and the computational time limit was set to 3,600 seconds. One indicator of model complexity is the number of binary variables involved in mathematical model, which was recorded in the second column and the seventh column. The upper bound (best known solution), lower bound, optimality gap and computational time (CPU time) were presented from the third column to sixth column and eighth to eleventh column, respectively.

The computational results presented in Tables 3 and 4 show that a large number of binary variables were involved in the mathematical models with under 4 discrete time interval settings. As shown in column "Binary Variables", the original discrete time model complexity grows as the planning period is lengthened and discrete time interval is reduced. Setting the discrete time interval as 60 minutes resulted in failure of creating a mathematical model, due to significant number of discrete time points along the entire planning period. Moreover, the branch-and-bound algorithm was not able to identify any feasible solutions for medium- and large-scale instances under short discrete time interval settings. It is noted that prescribing a large time interval gap between two consecutive time points may also drop down the real optimal solution, e.g., the time point leading to minimum operating and tardiness cost is eliminated at the model initialization stage. The branch-and-bound algorithm needs to identify the time point that is closest to the real optimal discrete time point eliminated by the model, which induces respective tardiness cost. The deviation of best-known solution under different model time interval settings exists when the stopping criterion was met or the optimality gap drops to zero. For example, the optimal solutions obtained by the original discrete time model across 4 different time interval settings for instance 1_5(1) are different, i.e. 60, 420, 869.91 and 3060, respectively. It is noted that the original discrete time model with the larger time interval delays the movement operations in hangar associates with a higher objective value.

The computational results under the same instances scale also reveal that the parameter settings of mission flights' arrival and cargo handling load are another significant determinant of problem complexity, in addition to the number of mission aircraft involved in problem and the length of planning period mentioned above. The arrival correlation between incoming flights also has impact on solution difficulties. If flights' arrival time concentrate into a short period, runway and hangar congestions will occur. Moreover, the extent of operation delays on runway and cargo hangar can worsen if mission flights arrive with complex cargo handling tasks, requiring more hangar capacity to accommodate the associated aircraft's parking requirements. For example, the computational results for 2_8(x) series instances were different. The "out of memory" outcomes were recorded for 2_8(1), 2_8(2) and 2_8(4) instances under the 30 minutes interval setting, indicating that the branch-and-bound algorithm by CPLEX was not able to initiate the MILP model given their complexity. Our further investigation reveals that the instances with the "out of memory" outcome have their problem setting configured with concentrated arrival of mission aircraft or long planning period. Large number of discrete time points were created in the planning horizon, requiring more branching effort in obtaining promising solutions. Moreover, the geometrical complexity associated with aircraft sizes also has impacted computational efficiency, as the hangar space becomes limited to accommodate all incoming large- or medium-sized mission aircraft.

To verify the effectiveness of the optimization model and methodology, the details of optimization results are extracted, including scheduled time and actual time of runway landing and departure and actual time of hangar roll in and roll out. We supplemented the details for three problem instances from normal congestion level to light/moderate congestion level, including 1_3(1), 2_8(2) and 3_9(3). The problem parameters of three instances are presented in Table 6, Table 8, and Table 10, respectively. The details of optimized results for three instances were reported in Table 7, Table 9, and Table 11, respectively. Departure delays were recorded under different interval settings, which implies a weak continuity between aircraft sequencing & scheduling and cargo hangar planning. Specifically, some aircraft cannot depart from the airport upon rolling out from the cargo hangar, inducing a time gap between roll out time and departure time.

By comparing the computational results with two-stage optimization method with model enhancement, it is found that the original model in this section cannot find the better solution, or the same solution as in the two-stage optimization approach. In this regard, we summarize the performance of the original model as follows:

1) Regarding the computational efficiency, the original model with short time interval (30 minutes, 60 minutes) settings has difficulties in initializing the MILP model, given the large number of discrete time points along the planning horizon (time frame) of problem instances.

Specifically, the number of discrete time points = length of planning horizon / time interval. Moreover, for problem instances with long time frame (planning horizon), updating solutions (also lower and upper bounds) in the original model becomes a great computational challenge or even intractable for the default branch-and-bound algorithm provided by CPLEX.

2) Regarding the solution quality, the original model with long time interval (60 minutes, 120 minutes, 300 minutes) settings may prune down the true optimal solution during the preprocessing phase, which induces actual delays of cargo flights.

For example, “60 minutes interval setting” creates discrete time point 0, 60, 120, 180, 240, …, along the planning horizon. If we know that the true optimal solution for a cargo flight’s roll out time is at the 110 mins time point, the original model with “60 minutes interval setting” would return the 120 mins time point as this cargo flight’s optimal roll out time, since the 110 mins time point does not exist in such model. In this regard, such cargo flight is forced to have 10 minutes delay under such “60 minutes interval setting”.

Table 4 Comparisons among basic discrete time models with different time interval settings

Instance	30 minutes interval					60 minutes interval				
	Binary Variables	Best-known solution	Lower bound	Gap	CPU (seconds)	Binary Variables	Best-known solution	Lower bound	Gap	CPU (seconds)
1_3(1)	23932	0	0	0	6.09	12113	180.00	180.00	0	6.64
1_4(1)	69806	0	0	0	16.44	35146	240.00	240.00	0	88.36
1_5(1)	306906	0	0	0	603.83	153820	300.00	300.0	0	393.20
2_6(1)	597560	0	0	0	3371.95	299300	360.00	360.00	0	1411.27
2_7(1)	out of memory	N/A	N/A	N/A	N/A	427821	420.00	420.00	0	2811.19
2_7(2)	out of memory	N/A	N/A	N/A	N/A	379007	1407.68	600.00	57.38	3600
2_7(3)	out of memory	N/A	N/A	N/A	N/A	135172	420.00	420.00	0	425.55
2_7(4)	out of memory	N/A	N/A	N/A	N/A	295366	4170.00	3659.98	12.23	3600
2_8(1)	out of memory	N/A	N/A	N/A	N/A	592254	N/A	450.86	N/A	3600
2_8(2)	out of memory	N/A	N/A	N/A	N/A	515865	N/A	328.04	N/A	3600
2_8(3)	out of memory	N/A	N/A	N/A	N/A	205259	480.00	480.00	0	1086.55
2_8(4)	out of memory	N/A	N/A	N/A	N/A	557159	N/A	492.78	N/A	3600
2_8(5)	out of memory	N/A	N/A	N/A	N/A	261343	885.00	885.00	0	1720.05
2_8(6)	out of memory	N/A	N/A	N/A	N/A	176061	300.00	300.00	0	1259.81
2_8(7)	out of memory	N/A	N/A	N/A	N/A	185986	566.24	480.00	15.23	3600

2_8(8)	out of memory	N/A	N/A	N/A	N/A	541819	420.00	150.91	64.07	3600
3_9(1)	out of memory	N/A	N/A	N/A	N/A	882016	N/A	182.03	N/A	3600
3_9(2)	out of memory	N/A	N/A	N/A	N/A	744477	N/A	567.02	N/A	3600
3_9(3)	out of memory	N/A	N/A	N/A	N/A	364719	540.00	540.00	0	2010.66
3_9(4)	out of memory	N/A	N/A	N/A	N/A	844836	N/A	522.45	N/A	3600
3_9(5)	out of memory	N/A	N/A	N/A	N/A	1735009	N/A	211.61	N/A	3600
3_9(6)	out of memory	N/A	N/A	N/A	N/A	402874	1031.00	1031.00	0	3114.20
3_9(7)	out of memory	N/A	N/A	N/A	N/A	717821	N/A	389.93	N/A	3600
3_9(8)	out of memory	N/A	N/A	N/A	N/A	544159	10004.00	151.58	98.48	3600
3_9(9)	out of memory	N/A	N/A	N/A	N/A	465020	N/A	420.03	N/A	3600
3_9(10)	out of memory	N/A	N/A	N/A	N/A	73335	585.00	585.00	0	115.83
3_10(1)	out of memory	N/A	N/A	N/A	N/A	1042125	N/A	299.00	N/A	3600
3_10(2)	out of memory	N/A	N/A	N/A	N/A	538043	N/A	479.98	N/A	3600
3_10(3)	out of memory	N/A	N/A	N/A	N/A	421266	N/A	387.58	N/A	3600

N/A: Not applicable

Table 5 Comparisons among basic discrete time models with different time interval settings

Instance	120 minutes interval					300 minutes interval				
	Binary Variables	Best-known solution	Lower bound	Gap	CPU (seconds)	Binary Variables	Best-known solution	Lower bound	Gap	CPU (seconds)
1_3(1)	6205	420.0	420.00	0	1.39	2564	1260.00	1260.00	0	0.44
1_4(1)	17734	690.00	690.00	0	8.78	7393	2040.00	2040.00	0	1.39
1_5(1)	77195	659.95	659.95	0	191.02	31225	2460.00	2460.00	0	10.69
2_6(1)	150238	1020.00	1020.00	0	423.51	60582	3120.00	3120.00	0	49.89
2_7(1)	214760	1020.20	1020.20	0	864.16	86608	3269.97	3269.97	0	103.64
2_7(2)	190018	1440.00	1440.00	0	658.75	76708	3660.00	3660.00	0	201.78
2_7(3)	68033	1380.00	1380.00	0	133.56	28009	4020.00	4020.00	0	7.00
2_7(4)	148285	4110.00	4110.00	0	474.47	60093	7290.00	7290.00	0	20.84
2_8(1)	297197	1139.80	1139.80	0	1324.42	120161	3600.00	3600.00	0	159.44
2_8(2)	258681	720.00	720.00	0	1884.14	104454	3750.00	3750.00	0	402.06
2_8(3)	103556	1560.00	1560.00	0	233.75	42216	4440.00	4440.00	0	66.25
2_8(4)	279408	N/A	971.93	N/A	3600	113243	4350.00	4350.00	0	177.58
2_8(5)	131880	1905.00	1905.00	0	463.72	53906	5726.00	5726.00	0	89.25
2_8(6)	89120	1260.00	1260.00	0	188.30	36454	3600.00	3600.00	0	5.58

2_8(7)	93557	1930.90	1930.90	0	387.66	38225	3720.00	3720.00	0	17.30
2_8(8)	271946	24660.00	1019.84	95.86	3600	109566	4740.00	4740.00	0	165.00
3_9(1)	441833	N/A	1349.74	N/A	3600	178430	4230.00	4230.00	0	457.89
3_9(2)	373779	119726.96	1196.90	99.00	3600	150578	3810.00	3810.00	0	635.22
3_9(3)	183135	1860.00	1860.00	0	813.50	74725	4980.00	4980.00	0	142.83
3_9(4)	423486	N/A	524.56	N/A	3600	170877	N/A	4589.95	N/A	3600
3_9(5)	868993	N/A	545.62	N/A	3600	349005	N/A	3749.70	N/A	3600
3_9(6)	202442	1931.00	1931.00	0	1011.58	82106	4691.00	4691.00	0	178.94
3_9(7)	359709	N/A	1019.79	N/A	3600	145064	6360.00	5160.00	18.87	3600
3_9(8)	272819	N/A	1424.80	N/A	3600	110135	4770.00	4770.00	0	306.91
3_9(9)	233257	N/A	1559.72	N/A	3600	94332	4620.00	4620.00	0	198.16
3_9(10)	37366	1740.00	1740.00	0	22.14	16206	5280.00	5280.00	0	4.33
3_10(1)	523019	N/A	1286.90	N/A	3600	210449	4590.00	4590.00	0	1063.39
3_10(2)	269943	N/A	1829.84	N/A	3600	110100	5040.00	5040.00	0	253.88
3_10(3)	211794	2171.00	2171.00	0	1022.95	86020	5771.00	5771.00	0	211.72

N/A: Not applicable

Table 6 Problem parameters of instance 1_3(1)

Flight ID	Estimated time of arrival (ETA)	Estimated time of departure (ETD)	Required Cargo Processing Time (CPT) (Hour:Minute)	Aircraft Type
1	29 December 17:30	3 January 17:00	119:30	G450
2	1 January 16:00	3 January 17:00	49:00	G450
3	4 January 09:30	7 January 17:00	79:30	G550

Table 7 Optimization results of instance 1_3(1), with 30 minutes interval setting

Flight ID	Landing time	Landing Runway	Roll in time to hangar	Roll out time from hangar	Departure time	Departure Runway	Delay (minutes)
1	29 Dec 17:30	1	29 Dec 17:30	3 Jan 17:00	3 Jan 17:00	1	0
2	1 Jan 16:00	0	1 Jan 16:00	3 Jan 17:00	3 Jan 17:00	0	0
3	4 Jan 9:30	0	4 Jan 9:30	7 Jan 17:00	7 Jan 17:00	0	0

Table 8 Problem parameters of instance 2_8(2)

Flight ID	Estimated time of arrival	Estimated time of departure	Required Cargo Processing Time (Hour:Minute)	Aircraft Type
1	15 January 18:00	30 January 17:00	359:00	G550
2	15 January 15:15	16 January 17:00	25:45	G550
3	16 January 11:30	17 January 17:00	29:30	G650
4	16 January 15:00	21 January 09:00	114:00	B738
5	21 January 23:55	22 January 08:00	8:05	A320
6	20 January 17:00	27 January 17:00	168:00	F900LX
7	12 January 22:30	14 January 10:30	36:00	A321
8	22 January 12:00	22 January 22:00	10:00	A332

Table 9 Optimization results of instance 2_8(2), with 120 minutes interval setting

Flight ID	Landing time	Landing Runway	Roll in time to hangar	Roll out time from hangar	Departure time	Departure Runway	Delay (minutes)
1	15 Jan 18:00	0	15 Jan 18:30	30 Jan 18:30	30 Jan 18:30	0	90
2	15 Jan 15:15	2	15 Jan 16:30	16 Jan 18:30	16 Jan 18:30	2	90
3	16 Jan 11:30	2	16 Jan 12:30	17 Jan 18:30	17 Jan 18:30	2	90
4	16 Jan 15:00	0	16 Jan 18:30	21 Jan 08:30	21 Jan 09:00	0	0
5	21 Jan 23:55	0	22 Jan 02:30	22 Jan 06:30	22 Jan 08:00	0	0
6	20 Jan 17:00	0	20 Jan 18:30	27 Jan 18:30	27 Jan 18:30	0	90
7	12 Jan 22:30	0	12 Jan 22:30	14 Jan 10:30	14 Jan 10:30	0	0
8	22 Jan 12:00	0	22 Jan 14:30	22 Jan 20:30	22 Jan 22:00	0	0

Table 10 Problem parameters of instance 3_9(3)

Flight ID	Estimated time of arrival	Estimated time of departure	Required Cargo Processing Time (Hour:Minute)	Aircraft Type
1	1 February 17:30	2 February 15:00	21:30	CL605
2	4 February 12:00	9 February 17:00	125:00	G450
3	6 February 14:00	10 February 17:00	99:00	F900LX
4	9 February 16:30	10 February 17:00	24:30	G5000
5	10 February 17:00	12 February 17:00	48:00	B737
6	11 February 19:00	13 February 17:00	46:00	G550
7	13 February 18:30	19 February 17:00	142:30	G550
8	13 February 19:30	15 February 18:00	46:30	G450
9	14 February 18:00	20 February 17:00	143:00	GL5T

Table 11 Optimization results of instance 3_9(3), with 300 minutes interval setting

Flight ID	Landing time	Landing Runway	Roll in time to hangar	Roll out time from hangar	Departure time	Departure Runway	Delay (minutes)
1	1 Feb 17:30	0	1 Feb 17:30	2 Feb 18:30	2 Feb 18:30	0	210
2	4 Feb 12:00	0	4 Feb 15:30	9 Feb 20:30	9 Feb 20:30	0	210
3	6 Feb 14:00	0	6 Feb 17:30	10 Feb 21:30	10 Feb 21:30	0	270
4	9 Feb 16:30	0	9 Feb 20:30	10 Feb 21:30	10 Feb 21:30	0	270
5	10 Feb 17:00	0	10 Feb 21:30	12 Feb 23:30	12 Feb 23:30	0	390
6	11 Feb 19:00	0	11 Feb 22:30	14 Feb 00:30	14 Feb 00:30	0	450
7	13 Feb 18:30	0	13 Feb 19:30	19 Feb 20:30	19 Feb 20:30	0	210
8	13 Feb 19:30	2	13 Feb 19:30	15 Feb 21:30	15 Feb 21:30	2	210
9	14 Feb 18:00	0	14 Feb 20:30	20 Feb 21:30	20 Feb 21:30	0	270

5.2.2 Evaluation of the proposed two-stage optimization method

The computational results in Section 5.2.1 demonstrate that the original discrete-time model with different time interval settings have difficulties in solving small and medium scale instances. Several instances cannot be solved to optimal while meeting the given time limit. The examination of the proposed two-stage optimization method is further conducted in this section. We examined the effectiveness of the second-stage enhancement proposed in Section 4.4, and compared with the original two-stage optimization without the enhancement. Our preliminary experiment suggested that setting the original discrete time interval of the second-stage problem as 60 minutes resulted in many "Out of Memory" outcomes when resolving medium and large-scale instances. In this connection, we prescribed the time interval in the original discrete time model as 120 minutes, considering the tradeoff between computational efficiency and solution outcome. The adjusted MILP models for the first-stage problem and the second-stage problem described in Sections 4.1 and 4.2 were solved by the branch-and-bound algorithm provided by CPLEX. For fair comparison, we prescribed the time limit for solving each subproblem as 1,800 seconds.

The computational results for the two-stage optimization method are reported in Table 5, presenting significant efficiency enhancement after adopting the second-stage model enhancement approach introduced in Section 4.4. Similar to Section 5.2.1, we recorded the number of binary variables involved in two subproblems to indicate the model complexity, in addition to the number of iterations run by the algorithm while meeting optimization stopping criteria. The model enhancement approach for the second-stage problem introduced in Section 4.4 outperforms the original discrete time model, regarding the solution quality objective value and computational efficiency CPU time. The high tardiness costs and mission flight rejection costs recorded in “Two-stage optimization with 120 minutes interval” column suggested that the true optimal solutions were pruned down by the original discrete time model, forcing mission flight’s operations delay in hangar. For the benefits from model decomposition and reorganization in two-stage optimization method, the connectivity between airside and groundside operations under a disaster relief scenario was enhanced by the embedded constraints and information exchange mechanism. As the searching space of each subproblem from the two-stage method has been narrowed down, the computational efforts in probing the logical association between numerous binary variables can be alleviated. The branch-and-bound algorithms used to solve the original discrete time mathematical model may trap into a series of unpromising solutions, while consuming a lot of resources in pruning the infeasible/unpromising branching trees during the search process. The length of logical chains connecting various binary variables is shorten by decomposition, then reconstructed by conveying critical decision information in airside and groundside operations in the optimization problem.

In particular, the efficiency of the proposed method benefits from the cargo handling time extension and airside and groundside operating decision exchange and adjustments. Specifically, the excessive parking demands and incapability of cargo accommodation can be clearly expressed with linear expression, rather than a combination of values of the binary variables controlling the operations decisions. A harmonious coordination of runway and cargo hangar resources is established afterwards by parallel adjustment of operations time windows. From the perspective of airport operations under disaster relief mode, addressing a large number of incoming mission flights is a common challenge under critical time in a practical situation. In view of efficiency and reliability in deriving a good quality solution, the propose method is able to address problem instances for practical uses, considering that the airport planner needs to have a ready-to-use solution under stressful environment and with limited decision-making time.

Similar to Section 5.2.1, we extract the details of the optimization results from three representative problem instances, namely 1_3(1), 2_8(2) and 3_9(3). The optimized schedules solved by the proposed two-stage optimization method with the model enhancement approach are reported in Table 13, Table 14 and Table 15, respectively. Compared to the results in Section 5.2.1, the proposed optimization method was able to eliminate the departure delays across three instances, manifesting its advantages in strengthening the relation between runway scheduling and cargo hangar planning.

As we did not differentiate the operating mode of each runway in the mathematical model, we would like to point out that it is possible that there are symmetric solutions leading to the same objective value for one problem instance, as shown in Table 14 and Table 9 for Instance 2(8)_2.

Specifically, we provide the following simple example to illustrate the idea of symmetric solution. The two different runway assignment solutions shown below are for the same problem instance, which lead to the same objective value on the condition that the roll in and roll out time are the same.

Solution 1:

Assignment of runway

Flight 1 to Runway 1 (Landing time 8:00 am), Flight 2 to Runway 1 (Landing time 8:10 am);

Flight 3 to Runway 2 (Landing time 8:00 am)

Solution 2:

Assignment of runway

Flight 3 to Runway 1 (Landing time 8:00 am)

Flight 1 to Runway 2 (Landing time 8:00 am), Flight 2 to Runway 2 (Landing time 8:10 am);

By comparing the computational results with the original model in different time interval settings, the two-stage optimization approach with model enhancement outperforms the original model, particularly the solution quality. In this regard, we summarize the performance of the two-stage optimization method as follows:

1) Regarding the computational efficiency, the advantages of model decomposition and reorganization in two-stage optimization method are manifested. By utilizing the information exchange mechanism between airside and groundside operations, the connectivity between airside and groundside operations decisions are enhanced. Furthermore, since we divide the original problem into two subproblems with strong connectivity, the searching space of each subproblem has been narrowed down. Therefore, the computational efforts in probing the logical association between numerous binary variables are alleviated, and the proposed optimization method is able to update better solutions with less time, enhancing the computational efficiency.

2) Regarding the solution quality, the two-stage optimization method reserves all possible arrival time, departure time, hangar roll in and hangar roll out time at the preprocessing phase. In this connection, the true optimal solution will not be pruned down as in the original model with different time interval settings.

Table 12 Computational performance of the two-stage optimization method

Instance	Two-stage optimization with 120 minutes interval					Two-stage optimization with model enhancements				
	Binary Variables in First Stage	Binary Variables in Second Stage	Iteration	Objective Value	CPU	Binary Variables in First Stage	Binary Variables in Second Stage	Iteration	Objective Value	CPU
1_3(1)	132	6166	1	46420.12	1.92	132	350	0	0	0.66
1_4(1)	224	17686	1	81420.12	5.79	224	1368	0	0	0.21
1_5(1)	340	77140	1	228380.12	130.21	340	2599	0	0	0.45
2_6(1)	480	150180	2	300100.12	94.19	480	6039	0	0	0.87
2_7(1)	644	214701	1	318180.12	532.25	644	14368	0	0	2.35
2_7(2)	644	189993	1	253420.00	651.00	644	31305	0	0	5.75
2_7(3)	644	67802	1	175080.02	55.25	644	11616	0	0	1.49
2_7(4)	644	148100	1	16242.000	571.55	644	40206	0	3540.00	7.74
2_8(1)	832	297133	1	335720.12	2069.84	832	36953	0	0	6.02
2_8(2)	832	258707	1	270170.00	1547.27	832	81329	0	0	17.32
2_8(3)	832	103304	1	191900.02	41.18	832	28810	0	0	4.01
2_8(4)	832	279414	0	223260.00	1794.04	832	98329	0	0	34.88
2_8(5)	832	131986	0	95280.00	30.93	832	32532	0	0	4.73
2_8(6)	832	89062	1	42370.00	123.34	832	17503	0	0	3.71
2_8(7)	832	93192	1	134374.00	123.31	832	14237	0	116.00	2.64

2_8(8)	832	271878	1	185240.61	1451.72	832	118287	0	0	24.89
3_9(1)	1044	441774	2	386560.12	2082.39	1044	89739	0	0	19.77
3_9(2)	1044	373836	1	301695.00	2756.90	1044	189103	0	0	38.43
3_9(3)	1044	182856	1	243460.02	504.43	1044	65655	0	0	12.50
3_9(4)	1044	423501	1	286790.02	3625.01	1044	243312	0	0	139.98
3_9(5)	1044	868915	out of memory			1044	412936	0	181.00	3625.19
3_9(6)	1044	202170	0	200995.16	531.20	1044	186355	0	138.00	35.98
3_9(7)	1044	359412	2	332760.00	3695.18	1044	110158	0	0	20.55
3_9(8)	1044	272475	1	214865.06	579.60	1044	310293	0	101.00	72.40
3_9(9)	1044	233016	1	230320.17	579.12	1044	237568	0	0	42.64
3_9(10)	1044	36855	1	89995.00	10.87	1044	5794	0	0	1.82
3_10(1)	1280	523113	1	205915.00	3650.19	1280	452670	0	0	542.75
3_10(2)	1280	269635	1	260230.00	801.79	1280	128327	0	0	28.08
3_10(3)	1280	211308	1	214515.00	527.86	1280	338241	0	221.00	66.79

Table 13 Optimization results of instance 1_3(1), solved by two-stage optimization & model enhancement

Flight ID	Landing time	Landing Runway	Roll in time to hangar	Roll out time from hangar	Departure time	Departure Runway	Delay (minutes)
1	29 Dec 17:30	0	29 Dec 17:30	3 Jan 17:00	3 Jan 17:00	0	0
2	1 Jan 16:00	1	1 Jan 16:00	3 Jan 17:00	3 Jan 17:00	1	0
3	4 Jan 09:30	2	4 Jan 09:30	7 Jan 17:00	7 Jan 17:00	2	0

Table 14 Optimization results of instance 2_8(2), solved by two-stage optimization & model enhancement

Flight ID	Landing time	Landing Runway	Roll in time to hangar	Roll out time from hangar	Departure time	Departure Runway	Delay (minutes)
1	15 Jan 18:00	1	15 Jan 18:00	30 Jan 17:00	30 Jan 17:00	1	0
2	15 Jan 15:15	1	15 Jan 15:15	16 Jan 17:00	16 Jan 17:00	1	0
3	16 Jan 11:30	0	16 Jan 11:30	17 Jan 17:00	17 Jan 17:00	0	0
4	16 Jan 15:00	1	16 Jan 15:00	21 Jan 09:00	21 Jan 09:00	1	0
5	21 Jan 23:55	1	21 Jan 23:55	22 Jan 08:00	22 Jan 08:00	1	0
6	20 Jan 17:00	0	20 Jan 17:00	27 Jan 17:00	27 Jan 17:00	0	0
7	12 Jan 22:30	0	12 Jan 22:30	14 Jan 10:30	14 Jan 10:30	0	0
8	22 Jan 12:00	1	22 Jan 12:00	22 Jan 22:00	22 Jan 22:00	1	0

Table 15 Optimization results of instance 2_8(2), solved by two-stage optimization & model enhancement

Flight ID	Landing time	Landing Runway	Roll in time to hangar	Roll out time from hangar	Departure time	Departure Runway	Delay (minutes)
1	1 Feb 17:30	0	1 Feb 17:30	2 Feb 15:00	2 Feb 15:00	0	0
2	4 Feb 12:00	0	4 Feb 12:00	9 Feb 17:00	9 Feb 17:00	0	0
3	6 Feb 14:00	0	6 Feb 14:00	10 Feb 17:00	10 Feb 17:00	0	0
4	9 Feb 16:30	0	9 Feb 16:30	10 Feb 17:00	10 Feb 17:00	0	0
5	10 Feb 17:00	0	10 Feb 17:00	12 Feb 17:00	12 Feb 17:00	0	0
6	11 Feb 19:00	0	11 Feb 19:00	13 Feb 17:00	13 Feb 17:00	0	0
7	13 Feb 18:30	1	13 Feb 18:30	19 Feb 17:00	19 Feb 17:00	1	0
8	13 Feb 19:30	0	13 Feb 19:30	15 Feb 18:00	15 Feb 18:00	0	0
9	14 Feb 18:00	0	14 Feb 18:00	20 Feb 17:00	20 Feb 17:00	0	0

6. Conclusions

This paper investigates airport operations management under post-disaster relief scenarios. Considering the concentrated aircraft traffic demand for relief cargo transportation within a short period of time, the accommodating capacities of the airport runway and cargo processing hangar should be coordinated properly. Any inefficient operations of runway and cargo hangar may cause dramatic loss and even disruption to airport under critical moment during post-disaster relief operating mode. Aircraft traffic and ground operations congestions are common during daily operations. The impact of aggregate congestions and delays should not be underestimated especially under post-disaster relief situations, as each incoming mission flight associated with relief cargo loading/unloading task is critical. In practice, each mission flight's expected arrival and departure time are planned according to its respective cargo transport needs, which generates peak hours spontaneously. In addition to limited runway resource, limited cargo hangar space is another critical bottleneck under relief cargo transportation scenarios, since the blockings of aircraft movement operations and difficulties in arranging mission aircraft with different physical sizes bring challenges in carrying out cargo hangar operation plans. We believe the integrated management of these two critical resources under relief cargo transportation scenarios enhances the resilience of airport operations and mitigates the tardiness caused by incoordination between critical airport operating resources.

The Mixed-Integer Linear Programming (MILP) model, which consolidates the operations of runway and cargo hangar, is introduced to develop an integrated airport operations management solution under the post-disaster operating mode. Regarding the solution procedures, the two-stage optimization method alleviates the computational complexity by creating subproblems that are equivalent to the original MILP model, and the local solutions of subproblems are coordinated and updated by additions of connecting constraints when iteration continues. The solution efficiency of the cargo hangar arrangement subproblem, i.e. the second-stage problem, is further enhanced by eliminating the unpromising discrete time points along the planning period according to the First-Come-First-Serve practice. The computational results demonstrated the efficiency and effectiveness of the proposed optimization method, which outperforms the pure branch-and-bound algorithm in regard to objective value and computational time. Through a systematic integrated management of runway and cargo hangar resources, the tardiness caused by incoordination between the aircraft sequencing and scheduling on runway and the parking arrangement in cargo hangar can be avoided, enhancing the turnover rate of mission flights during the post-disaster relief situation.

For further research on this topic, several aspects can be considered. Firstly, we suggest extending the current model to incorporate uncertainty in aircraft sequencing and scheduling on runway, as extreme weather conditions may affect the quality of implementing the solution through airport operations. Secondly, the application of the proposed model can be extended to other scenarios. For example, cargo hangar arrangement and runway scheduling problem are common at the hub airports for freighter operators, such as Louisville (SDF) airport for UPS and Memphis (MEM) airport for FedEx. Furthermore, an integration of deicing pad assignment and runway scheduling problem can be considered, replacing the cargo hangar arrangement with deicing zone assignment. Furthermore, some assumptions can be eliminated, so as to generalize the model for applications. Thirdly, emergency flights may arrive during airport operations, and priority changes on landing and cargo processing in hangar are possible. Therefore, the impact of airport operations reschedule on other stakeholder's interests can be taken into consideration, which enhances the applicability of the proposed airport management methodology.

References

[1] X. Gao, X. Jin, P. Zheng, C. Cui, Multi-modal transportation planning for multi-commodity rebalancing under uncertainty in humanitarian logistics, Advanced Engineering Informatics, 47 (2021) 101223.
[2] D.T. Aksu, L. Ozdamar, A mathematical model for post-disaster road restoration: Enabling accessibility and evacuation, Transportation Research Part E-Logistics and Transportation Review, 61 (2014) 56-67.
[3] E. Dufour, G. Laporte, J. Paquette, M.-E. Rancourt, Logistics service network design for humanitarian response in East Africa, Omega-International Journal of Management Science, 74 (2018) 1-14.
[4] A. Moreno, D. Alem, D. Ferreira, Heuristic approaches for the multiperiod location-transportation problem with reuse of vehicles in emergency logistics, Comput. Oper. Res., 69 (2016) 79-96.
[5] K.K.H. Ng, C.K.M. Lee, S.Z. Zhang, K. Wu, W. Ho, A multiple colonies artificial bee colony algorithm for a capacitated vehicle routing problem and re-routing strategies under time-dependent traffic congestion, Computers & Industrial Engineering, 109 (2017) 151-168.
[6] Y.-J. Zheng, H.-F. Ling, X.-L. Xu, S.-Y. Chen, Emergency scheduling of engineering rescue tasks in disaster relief operations and its application in China, International Transactions in Operational Research, 22 (2015) 503-518.
[7] H. Hu, K.K.H. Ng, Y. Qin, Robust Parallel Machine Scheduling Problem with Uncertainties and Sequence-Dependent Setup Time, Scientific Programming, 2016 (2016) 13.
[8] C.K.M. Lee, K.K.H. Ng, H.K. Chan, K.L. Choy, W.C. Tai, L.S. Choi, A multi-group analysis of social media engagement and loyalty constructs between full-service and low-cost carriers in Hong Kong, Journal of Air Transport Management, 73 (2018) 46-57.
[9] F. Li, C.-H. Lee, C.-H. Chen, L.P. Khoo, Hybrid data-driven vigilance model in traffic control center using eye-tracking data and context data, Advanced Engineering Informatics, 42 (2019) 100940.
[10] G. Xu, X. Qiu, M. Fang, X. Kou, Y. Yu, Data-driven operational risk analysis in E-Commerce Logistics, Advanced Engineering Informatics, 40 (2019) 29-35.
[11] Y. Yu, C. Yu, G. Xu, R.Y. Zhong, G.Q. Huang, An operation synchronization model for distribution center in E-commerce logistics service, Advanced Engineering Informatics, 43 (2020) 101014.
[12] C.K. Lee, S. Zhang, K.K. Ng, Design of An Integration Model for Air Cargo Transportation Network Design and Flight Route Selection, Sustainability, 11 (2019) 5197.
[13] K.K.H. Ng, C.K.M. Lee, F.T.S. Chan, Y. Lv, Review on meta-heuristics approaches for airside operation research, Applied Soft Computing, 66 (2018) 104-133.
[14] K.K.H. Ng, C.K.M. Lee, Makespan minimization in aircraft landing problem under congested traffic situation using modified artificial bee colony algorithm, 2016 IEEE International Conference on Industrial Engineering and Engineering Management (IEEM), IEEE, Bali, Indonesia, 2016, pp. 750-754.
[15] H. Lee, G. Li, A. Rai, A. Chattopadhyay, Real-time anomaly detection framework using a support vector regression for the safety monitoring of commercial aircraft, Advanced Engineering Informatics, 44 (2020) 101071.

[16] K.K.H. Ng, C.-H. Chen, C.K.M. Lee, Mathematical programming formulations for robust airside terminal traffic flow optimisation problem, Computers & Industrial Engineering, 154 (2021) 107119.
[17] K.K.H. Ng, C.K.M. Lee, F.T.S. Chan, Y. Qin, Robust aircraft sequencing and scheduling problem with arrival/departure delay using the min-max regret approach, Transportation Research Part E: Logistics and Transportation Review, 106 (2017) 115-136.
[18] K.K.H. Ng, C.K.M. Lee, A modified Variable Neighborhood Search for aircraft Landing Problem, 2016 IEEE International Conference on Management of Innovation and Technology (ICMIT), IEEE, Bangkok, Thailand, 2016, pp. 127-132.
[19] A. Salehipour, M. Modarres, L.M. Naeni, An efficient hybrid meta-heuristic for aircraft landing problem, Comput. Oper. Res., 40 (2013) 207-213.
[20] K.K.H. Ng, C.-H. Chen, C.K.M. Lee, J. Jiao, Z.-X. Yang, A systematic literature review on intelligent automation: Aligning concepts from theory, practice, and future perspectives, Advanced Engineering Informatics, 47 (2021) 101246.
[21] L. Bu, C.-H. Chen, G. Zhang, B. Liu, G. Dong, X. Yuan, A hybrid intelligence approach for sustainable service innovation of smart and connected product: A case study, Advanced Engineering Informatics, 46 (2020) 101163.
[22] K.K.H. Ng, C.K.M. Lee, F.T.S. Chan, Y.C. Qin, Robust aircraft sequencing and scheduling problem with arrival/departure delay using the min-max regret approach, Transportation Research Part E-Logistics and Transportation Review, 106 (2017) 115-136.
[23] A. Salehipour, An algorithm for single- and multiple-runway aircraft landing problem, Mathematics and Computers in Simulation, 175 (2020) 179-191.
[24] N.R. Sabar, G. Kendall, An iterated local search with multiple perturbation operators and time varying perturbation strength for the aircraft landing problem, Omega-International Journal of Management Science, 56 (2015) 88-98.
[25] K.K.H. Ng, C.K.M. Lee, F.T.S. Chan, C.-H. Chen, Y. Qin, A two-stage robust optimisation for terminal traffic flow problem, Applied Soft Computing, 89 (2020) 106048.
[26] K. Ng, C. Lee, F.T. Chan, An Alternative Path Modelling Method for Air Traffic Flow Problem in Near Terminal Control Area, 2019 2nd International Conference on Intelligent Autonomous Systems (ICoIAS), IEEE, 2019, pp. 171-174.
[27] K. Ng, C.K. Lee, Aircraft scheduling considering discrete airborne delay and holding pattern in the near terminal area, International Conference on Intelligent Computing, Springer, 2017, pp. 567-576.
[28] K.K.H. Ng, C.K.M. Lee, F.T.S. Chan, A robust optimisation approach to the aircraft sequencing and scheduling problem with runway configuration planning, 2017 IEEE International Conference on Industrial Engineering and Engineering Management (IEEM), IEEE, Singapore, Singapore, 2017, pp. 40-44.
[29] K.K.H. Ng, M.H.M. Tang, C.K.M. Lee, Design and development of a performance evaluation system for the aircraft maintenance industry, 2015 IEEE International Conference on Industrial Engineering and Engineering Management (IEEM), IEEE, Singapore, Singapore, 2015, pp. 564-568.
[30] X. Gao, P. Pishdad-Bozorgi, BIM-enabled facilities operation and maintenance: A review, Advanced Engineering Informatics, 39 (2019) 227-247.
[31] G. Chen, W. He, L.C. Leung, T. Lan, Y. Han, Assigning licenced technicians to maintenance tasks at aircraft maintenance base: a bi-objective approach and a Chinese airline application, International Journal of Production Research, (2017) 1-14.
[32] Y. Qin, F.T.S. Chan, S.H. Chung, T. Qu, B. Niu, Aircraft parking stand allocation problem with safety consideration for independent hangar maintenance service providers, Computers & Operations Research, (2017).
[33] S. Zheng, Z. Yang, Z. He, N. Wang, C. Chu, H. Yu, Hybrid simulated annealing and reduced variable neighbourhood search for an aircraft scheduling and parking problem, International Journal of Production Research, (2019) 1-21.
[34] E.E. Zachariadis, C.D. Tarantilis, C.T. Kiranoudis, The Vehicle Routing Problem with Simultaneous Pick-ups and Deliveries and Two-Dimensional Loading Constraints, European Journal of Operational Research, 251 (2016) 369-386.

[35] L.J. Wei, Z.Z. Zhang, D.F. Zhang, A. Lim, A variable neighborhood search for the capacitated vehicle routing problem with two-dimensional loading constraints, European Journal of Operational Research, 243 (2015) 798-814.
[36] F. Chang, G. Zhou, W. Cheng, C. Zhang, C. Tian, A service-oriented multi-player maintenance grouping strategy for complex multi-component system based on game theory, Advanced Engineering Informatics, 42 (2019) 100970.
[37] B. Cheang, X. Gao, A. Lim, H. Qin, W.B. Zhu, Multiple pickup and delivery traveling salesman problem with last-in-first-out loading and distance constraints, European Journal of Operational Research, 223 (2012) 60-75.
[38] J.F. Cote, M. Gendreau, J.Y. Potvin, An Exact Algorithm for the Two-Dimensional Orthogonal Packing Problem with Unloading Constraints, Operations Research, 62 (2014) 1126-1141.
[39] M. Cherkesly, G. Desaulniers, G. Laporte, A population-based metaheuristic for the pickup and delivery problem with time windows and LIFO loading, Comput. Oper. Res., 62 (2015) 23-35.
[40] S. Tyagi, N. Shukla, S. Kulkarni, Optimal design of fixture layout in a multi-station assembly using highly optimized tolerance inspired heuristic, Applied Mathematical Modelling, 40 (2016) 6134-6147.
[41] M. Mohammadi, K. Forghani, A novel approach for considering layout problem in cellular manufacturing systems with alternative processing routings and subcontracting approach, Applied Mathematical Modelling, 38 (2014) 3624-3640.
[42] M. Bagheri, M. Bashiri, A new mathematical model towards the integration of cell formation with operator assignment and inter-cell layout problems in a dynamic environment, Applied Mathematical Modelling, 38 (2014) 1237-1254.
[43] A. Ahmadi, M.R.A. Jokar, An efficient multiple-stage mathematical programming method for advanced single and multi-floor facility layout problems, Applied Mathematical Modelling, 40 (2016) 5605-5620.
[44] Y.A. Bozer, S.C. Rim, A branch and bound method for solving the bidirectional circular layout problem, Applied Mathematical Modelling, 20 (1996) 342-351.
[45] C. Chen, Y. Liu, S. Wang, X. Sun, C. Di Cairano-Gilfedder, S. Titmus, A.A. Syntetos, Predictive maintenance using cox proportional hazard deep learning, Advanced Engineering Informatics, 44 (2020) 101054.
[46] J.A. Bennell, J.F. Oliveira, The geometry of nesting problems: A tutorial, European Journal of Operational Research, 184 (2008) 397-415.
[47] J.A. Bennell, J.F. Oliveira, A tutorial in irregular shape packing problems, Journal of the Operational Research Society, 60 (2009) S93-S105.
[48] R. Alvarez-Valdes, A. Martinez, J.M. Tamarit, A branch & bound algorithm for cutting and packing irregularly shaped pieces, International Journal of Production Economics, 145 (2013) 463-477.
[49] M. Fischetti, I. Luzzi, Mixed-integer programming models for nesting problems, Journal of Heuristics, 15 (2009) 201-226.
[50] A. Martinez-Sykora, R. Alvarez-Valdes, J. Bennell, J.M. Tamarit, Constructive procedures to solve 2-dimensional bin packing problems with irregular pieces and guillotine cuts, Omega-International Journal of Management Science, 52 (2015) 15-32.
[51] L.H. Cherri, L.R. Mundim, M. Andretta, F.M.B. Toledo, J.F. Oliveira, M.A. Carravilla, Robust mixed-integer linear programming models for the irregular strip packing problem, European Journal of Operational Research, 253 (2016) 570-583.
[52] Y. Qin, Z.X. Wang, F.T.S. Chan, S.H. Chung, T. Qu, A mathematical model and algorithms for the aircraft hangar maintenance scheduling problem, Applied Mathematical Modelling, 67 (2019) 491-509.
[53] IBM, ILOG CPLEX Optimization Studio 20.1.0 CP Optimizer, https://www.ibm.com/docs/en/icos/20.1.0?topic=cp-optimizer